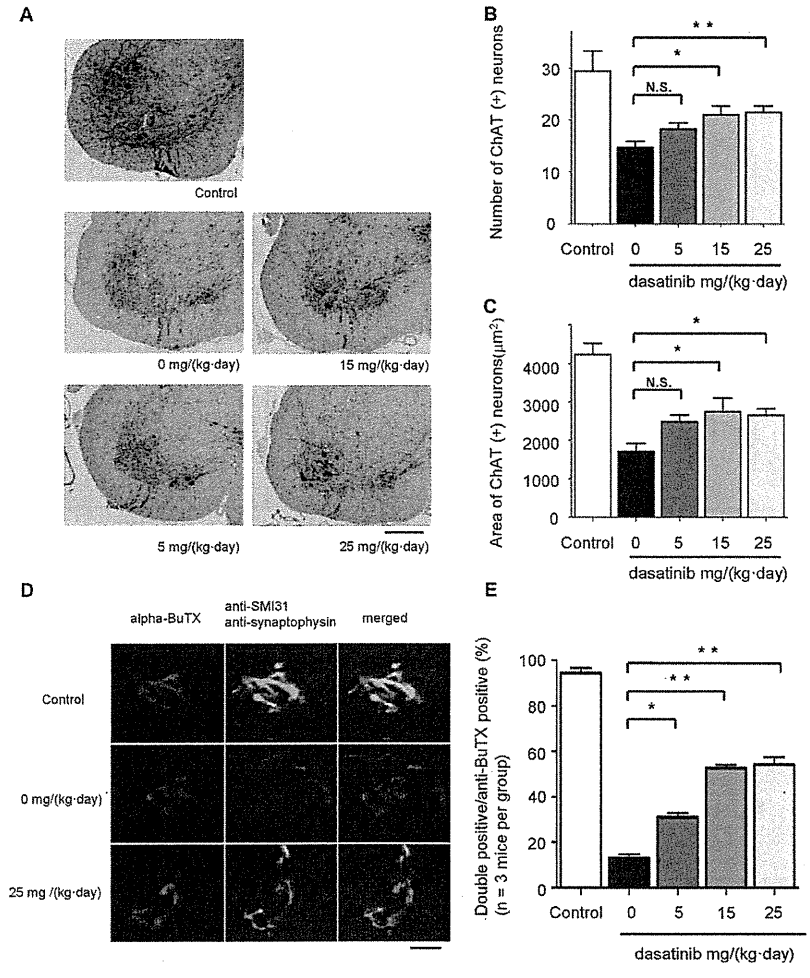

Figure 6. The effect of dasatinib on motor neuron survival in G93A mice. A: Spinal cord (L1-3) specimens from 120-day-old mice were immunostained with anti-ChAT antibody. The mice were administered the indicated amounts of dasatinib daily from postnatal day 56 to day 120 (n = 8 mice per group). Scale bar: 250 μm. B: The number of ChAT-positive neurons in the sections described in Fig. 6A was counted using Image J software. Dasatinib prevented the loss of ChAT-positive motor neurons in the ventral horn of G93A mice at doses of 15 mg/(kg·day) ($P<0.05$) and 25 mg/(kg·day) ($P<0.01$). Statistics were evaluated using 1-way ANOVA with Dunnett's post-hoc test. *$P<0.05$, **$P<0.01$. C: The area of ChAT-positive neurons in the sections described in Fig. 6A was determined using Image J software. Dasatinib increased the size of motor neuron cell bodies at doses of 15 and 25 mg/(kg·day) ($P<0.05$). Statistics were evaluated using 1-way ANOVA with Dunnett's post-hoc test. *$P<0.05$. D: To investigate the innervation status of NMJs, frozen quadriceps femoris specimens from 120-day-old mice were stained with alpha-BuTX (red) and anti-synaptophysin (green) or anti-SMI31 (green) antibodies. Representative NMJs visualized with the confocal laser scanning microscopy are shown. The mice were administered the indicated amounts of dasatinib daily from postnatal day 56 to day 120. Scale bar: 10 μm. E: The ratio of double-immunostained innervated NMJs to total NMJs is summarized. One hundred immunostained NMJs were investigated in each dasatinib-treated mouse (n = 3 mice per group). Dasatinib significantly ameliorated the destruction of NMJ innervation in G93A mice at doses of 5 ($P<0.05$), 15, and 25 mg/(kg·day) ($P<0.01$). Statistics were evaluated using 1-way ANOVA with Dunnett's post-hoc test. *$P<0.05$, **$P<0.01$.
doi:10.1371/journal.pone.0046185.g006

mice, hyperphosphorylation and upregulation of c-Abl was apparent in the lumbar spinal cord. Notably, although apoptosis-related molecules such as c-Abl were expected to exert their function at a relatively late stage of disease [34,35], the expression of c-Abl was increased at the presymptomatic stage. This unexpected result suggests that c-Abl may be an early player in the apoptotic cascade of ALS pathogenesis and thus a promising target to protect motor neurons against cytotoxic insults.

The currently available c-Abl inhibitors are imatinib, dasatinib, and nilotinib, all of which have been used for the treatment of CML, Ph+ALL, and gastrointestinal stromal tumor [36,37,38]. A number of studies have reported CNS relapse in patients treated with imatinib, which has poor BBB permeability [39,40,41,42,43,44], while in contrast, Porkka et al. reported that dasatinib crossed the BBB and showed therapeutic efficacy against CNS CML tumors in a mouse model and in patients with CNS leukemia (Ph+ALL) [45]. The high BBB permeability of dasatinib is advantageous for the treatment of ALS, since it is expected to achieve a sufficient therapeutic concentration in the CNS. We demonstrated that dasatinib at a dose of 15 mg/(kg·day) or more delayed disease progression and extended the survival of G93A mice. Immunostaining of spinal cords clearly demonstrated a dose-dependent protective effect of dasatinib on motor neuron survival by inhibiting apoptosis. These results indicate that c-Abl plays an

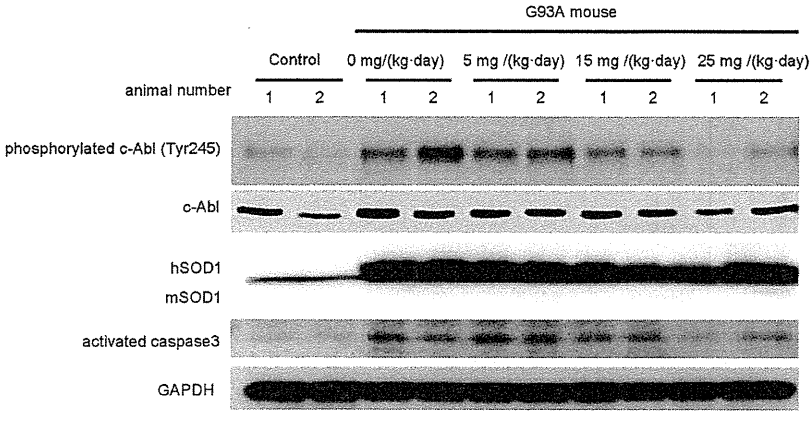

Figure 7. Dasatinib inhibits c-Abl phosphorylation in G93A mice. Protein levels of phosphorylated c-Abl (Tyr245), c-Abl, and activated caspase-3 were measured by western blot analysis using spinal cords from dasatinib- and vehicle-treated G93A mice (120 days old). GAPDH is shown as the loading control. hSOD1 and mSOD1 indicate human SOD1 and mouse endogenous SOD1, respectively. Western blot analysis is shown in duplicate. The animal number refers to individual animals. Parallel declines in c-Abl phosphorylation and activated caspase 3 were observed.
doi:10.1371/journal.pone.0046185.g007

important role in the disease pathogenesis of ALS in G93A mice and is a promising therapeutic target for ALS.

Since the involvement of c-Abl upregulation and activation has been demonstrated in neuronal cell apoptosis [46,47], we investigated whether upregulation of c-Abl is associated with an increased level of activated caspase-3, which correlates with apoptosis. Our results clearly showed that caspase 3 was activated in the spinal cords of G93A mice. Administration of dasatinib attenuated both c-Abl phosphorylation and caspase-3 activation in a dose-dependent manner. Thus, our results suggest that dasatinib ameliorates the phenotype of these animals by suppressing apoptotic cell death of motor neurons caused by mutant SOD1.

The examination of NMJs revealed that dasatinib successfully reversed the deinnervation of NMJs, an early pathological change reflecting motor neuron degeneration in mutant SOD1-mediated ALS [48]. Since levels of total and active c-Abl were increased in the spinal cords of G93A mice at the early stage of the disease (Fig. 4), dasatinib appears to improve NMJ function via c-Abl-mediated signaling. These findings suggest that dasatinib improved motor neuron function leading to amelioration of weight loss in G93A mice. They also demonstrate that the loss of synaptic contacts is a sensitive indicator of the beneficial effects exerted by dasatinib in G93A mice.

One possible explanation for the relatively small effects of dasatinib in this study is that the beneficial effects of this therapy on apoptosis were limited in motor neurons and could not reverse the physical dysfunction of the mice, despite the improvement in innervation at NMJs. Alternatively, dasatinib may not be capable of mitigating non-apoptotic pathways of motor neuron degeneration caused by mutant SOD1, since non-apoptotic programmed cell death has also been implicated in motor neuron damage in G93A mice [49]. Taken together, dasatinib may mitigate apoptotic events that occur at an early stage of the disease and partially improve motor neuron function via activation of c-Abl.

Using human postmortem spinal cord tissue, we demonstrated a significant increase in c-Abl expression in the spinal cord of sALS compared with non-ALS. Histochemical findings confirmed that c-Abl protein increased mainly in motor neurons. In addition, c-Abl phosphorylation was also increased in motor neurons in the affected area. These findings indicate that c-Abl abnormality is involved in human sALS cases as well as cellular and animal models of ALS. Thus far, not many drug candidates derived from research using mutant SOD1 transgenic animals have been successful in clinical trials for human sALS [50]. The implication of c-Abl in sALS as well as mutant SOD1-associated ALS supports the possible application of dasatinib as a candidate drug for sALS treatment. Our study showed that dasatinib treatment suppressed apoptosis and delayed disease progression in G93A mice, suggesting that dasatinib has a potential therapeutic value in humans, since apoptosis appears to be an important target of treatment development for ALS [35,51].

In conclusion, the major findings of this study are (1) the observation of c-Abl upregulation and activation in the spinal cords of G93A mice at a relatively early stage of the disease; (2) the improved survival of G93A mice with concomitant suppression of c-Abl phosphorylation and caspase-3 activation upon administration of a BBB-permeable c-Abl inhibitor, dasatinib; and (3) increased c-Abl expression and phosphorylation in postmortem spinal cord tissues from sALS patients. Taken together, our results suggest that c-Abl is a novel therapeutic target for ALS.

Materials and Methods

Cell lines

The mouse motor neuron hybridoma line NSC-34 was provided by Dr. N.R. Cashman (University of Toronto; Toronto, Canada) [30]. Human wild-type and mutant (G93A and G85R) SOD1 cDNAs were subcloned from pcDNA3.1/SOD1 into lentiviral expression vectors (pLenti-CMV/TO, kind gifts from Dr. Eric Campeau at the University of Massachusetts Medical School) [52]. Lentiviral particles were produced in HEK293T cells (Open Biosystems, Huntsville, AL, USA) by transfection with Lipofectamine 2000 (Invitrogen, Eugene, OR, USA). Lentivirus-containing supernatant was collected 48 h after transfection and stored at −80°C. Details of the lentivirus system have been described previously [52]. We first transduced the Tet repressor into NSC-34 cells and selected a single clone (NSC-34-TetR14) that demonstrated good induction without leaky expression. NSC-34-TetR14 cells were stably transduced with lentivirus-Tet-on/SOD1, an inducible lentivirus expressing Myc-tagged wild-type or mutant SOD1.

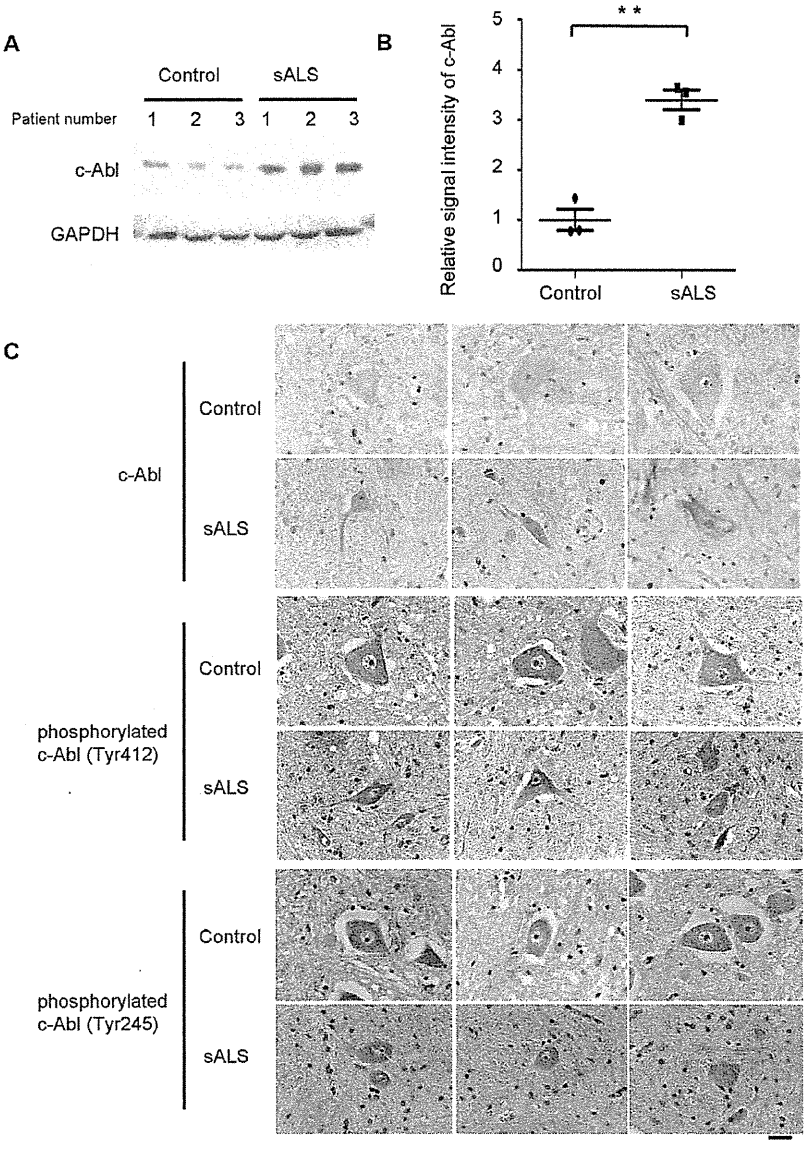

Figure 8. c-Abl upregulation and activation in affected motor neurons of sporadic ALS patients. A: The protein expression of total c-Abl was measured by western blot analysis using an anti-c-Abl antibody and the lumbar spinal cord tissue from sporadic ALS (sALS) cases and controls. GAPDH is shown as an internal control. The patient number refers to individual patients. B: Densitometric analysis using Image J software revealed a significant difference in the amount of total c-Abl protein in the lumbar spinal cords of sALS patients and controls ($P<0.01$). Data are presented as mean ± SEM. Statistical analysis was performed using Student's *t* test. $^{**}P<0.01$. C: Immunohistochemical analysis using paraffin-embedded spinal cords from control and sALS patients was carried out by staining with anti-c-Abl, anti-phosphorylated c-Abl (Tyr412), and anti-phosphorylated c-Abl (Tyr245) antibodies. Scale bar: 50 μm.
doi:10.1371/journal.pone.0046185.g008

Cell culture

NSC-34 cells were grown in Dulbecco's modified Eagle's medium (DMEM) containing 10% fetal calf serum (FCS; Invitrogen). The tet-on inducible cell lines were grown in DMEM supplemented with 10% tetracycline-free FCS (Clontech, Mountain View, CA, USA). All cell lines used in this study were cultured at 37°C in an atmosphere of 5% CO_2. We induced hSOD1 expression by adding 2 μg/ml doxycycline (Clontech) to the culture medium for the last 48 h of culture.

Cell viability assay

Each of the cell lines (3,500 cells per well) were grown on collagen-coated 96-well plates with serum-free medium. MTS (3-(4,5-dimethylthiazol-2-yl)-5-(3-carboxymethoxyphenyl)-2-(4-sulfophenyl)-2H-tetrazolium)-based cell proliferation assays were performed after 48 h of induction with doxycycline (Dox, 2 μg/ml) using the CellTiter 96® AQueous One Solution Cell Proliferation Assay (Promega, Madison, WI, USA). Briefly, we added CellTiter 96® AQueous One Solution Reagent to each well of a 96-well assay plate containing the samples in culture medium. After incubation at 37°C for 1 h, absorbance at 490 nm was measured

using a multiple-plate reader (Powerscan HT, Dainippon Pharmaceutical, Osaka, Japan), with assays carried out in triplicate.

Cytotoxicity detection assay

Cell injury was quantitatively assessed by measurement of LDH released from damaged or destroyed cells into the extracellular fluid after 48-h induction of wild-type or mutant SOD1. The activity of LDH released into the culture medium was measured with a Cytotoxicity Detection kit (Roche Applied Science, Burgess Hill, UK) according to the manufacturer's protocol. Briefly, after 48 h of induction with doxycycline (Dox, 2 μg/ml), we added substrate mixture from the kit to each well of a 96-well assay plate containing the culture supernatant. Following incubation for 30 min, absorbance at 490 nm was measured using a multiple-plate reader (Powerscan HT, Dainippon Pharmaceutical, Osaka, Japan).

Transgenic mice

Transgenic mice overexpressing the human SOD1 gene carrying the G93A mutation were purchased from the Jackson Laboratory (Bar Harbor, ME, USA) and maintained as hemizygotes by mating transgenic males with B6/SJLF1 females [53]. All animal experiments were performed in accordance with the National Institute of Health Guide for the Care and Use of Laboratory Animals and were approved by the Nagoya University Animal Experiment Committee.

Chemicals

Dasatinib was provided by Bristol-Myers Squibb. Propylene glycol was purchased from Sigma Chemical Co. (St Louis, MO, USA). SU6656 was purchased from Calbiochem (Darmstadt, Germany). All other chemicals used were reagent grade or better.

Drug formulation and administration

For oral administration, dasatinib was dissolved in a mixture of propylene glycol/water (50:50). The administration volume was 0.01 ml/g. Ludolph et al. recommended that a total of 48 G93A mice should be used in a preclinical trial if 2 groups (treated animals and controls; n = 24 per group) are to be compared, and recommended that the number of animals should be increased for testing the dose-response effect of a drug [50]. Therefore, we allocated 28 mice to each treatment group for the survival analysis. From postnatal day 56, dasatinib was administered by oral gavage using a 5-days-on/2-days-off once-daily schedule (Monday through Friday) at doses of 5, 15, and 25 mg/(kg·day). Control mice received vehicle alone.

Immunohistochemistry

Under pentobarbital anesthesia, mice were transcardially perfused with 20 ml phosphate buffer (pH 7.4). Tissues were postfixed overnight in 10% phosphate-buffered formalin and processed for paraffin embedding as previously described [54]. Transverse sections of spinal cord (6-μm thickness) were then deparaffinized with alcohol, rehydrated, and microwaved in 0.1 M citrate buffer (pH 6) as a pretreatment for antigen retrieval. Immunostaining was performed using the EnVision+ System-HRP (Dako, Glostrup, Denmark). Tissue sections were incubated with anti-c-Abl antibody (Abcam, Cambridge, MA) and anti-phospho-c-Abl (Tyr412 or Tyr245) antibody (Cell Signaling Technology, Beverly, MA, USA), both diluted 1:100 in Dako antibody diluent (Dako) for immunohistochemical analysis. Counterstaining was performed using hematoxylin. For fluorescence microscopic analysis, after antigen retrieval, tissue sections were incubated with TNB-buffer (0.10 M Tris-HCl, 0.15 M NaCl, 0.5% BMP) for 30 min at room temperature to block non-specific antibody binding. Then spinal tissue sections were incubated with anti-phospho-c-Abl (Tyr412 or Tyr245) antibody (Cell Signaling Technology), both diluted 1:100 in phosphate buffered saline (PBS) buffer, overnight at 4°C. After incubation with primary antibody, the sections were exposed to an appropriate secondary antibody conjugated to fluorescent dye and Topro-3 (Invitrogen) for 1 h at room temperature. Sections were visualized using a confocal microscope (LSM 710, Carl Zeiss, Oberkochen, Germany) under epifluorescent illumination. The intensity of immunostained neurons was semi-quantified using NIH Image J software (v 1.44, NIH, Bethesda, MD, USA).

Assessment of motor function

The motor performance of mice was assessed weekly using an Economex Rotarod (Columbus Instruments, Columbus, OH, USA) starting at 42 days of age. Staying on the rod for more than 180 s was considered to be the normal performance level, as previously described [55].

Western blot analyses

The spinal cords of dasatinib- and vehicle-treated mice were collected approximately 3 h after the final oral administration. Human and mouse spinal cords were snap frozen in liquid nitrogen, homogenized in ice-cold Cell Lytic-M Mammalian Cell Lysis/Extraction Reagent (Sigma), and centrifuged at 18,800× *g* for 15 min at 4°C. Protein concentration was determined by DC protein assay (Bio-Rad, Hercules, CA, USA). Western blotting was performed using standard procedures as described previously [56,57]. Primary antibodies were used at the following concentrations: anti-SOD1, 1:2,000 (Abcam); anti-Myc, 1:1,000 (MBL, Nagoya, Japan); anti-tubulin, 1:1,000 (Sigma); anti-c-Abl, 1:1,000 (BD Transduction); anti-phospho-c-Abl (Tyr412), 1:1,000 (Sigma); anti-phospho-c-Abl (Tyr245), 1:1000 (Cell Signaling Technology); anti-glyceraldehyde-3-phosphate dehydrogenase (GAPDH), 1:1,000 (Millipore, Billerica, MA); anti-phospho-c-Src (Tyr416), 1:1,000 (Cell Signaling Technology); anti c-Src, 1:1,000 (Cell Signaling Technology); and anti-cleaved caspase-3 (Asp175), 1:1,000 (Cell Signaling Technology). Secondary antibody probing and detection were performed using the ECL Plus kit (GE Healthcare, Buckinghamshire, UK). For detection of phosphorylated c-Abl, antibody was diluted in Tris-buffered saline (TBS) with Tween (0.5%) containing 3% BSA, otherwise 5% fat-free milk in TBS with Tween (0.5%) was used as the antibody dilutant. Chemiluminescence signals were digitalized (LAS-3000 Imaging System; Fujifilm, Tokyo, Japan), and band intensities were quantified using Multi Gauge software version 3.0 (Fujifilm).

Quantitative real-time PCR

Real-time PCR was performed as described previously [58]. In brief, total RNA from either mouse spinal cord or NSC-34 cells was reverse transcribed into first-strand cDNA using SuperScript II reverse transcriptase (Invitrogen). Real-time PCR was performed using QuantiTect SYBR Green PCR Master Mix and 0.4 M of each primer (Qiagen, Valencia, CA, USA), and the product was detected using the CFX96™ real-time system (Bio-Rad Laboratories). The reaction conditions were 95°C for 15 min, followed by 40 cycles of 15 s at 94°C, 30 s at 55°C, and 30 s at 72°C. The expression level of GAPDH was quantified and used as an internal standard control. The primers used were 5′-TCGTTACCTCCAAAGGCTGCTC-3′ and 5′-ATGGCGGTGTCTGGCTATTCA-3′ for c-Abl and 5′-TCAA-

GAAGGTGGTGAAGCAG-3′ and 5′-GTTGAAGTCGCAG-GAGACAA-3′ for GAPDH.

Motor neuron assessment by immunohistochemical analysis

At age 120 days, 8 animals from each treatment group were sacrificed, and the lumbar spinal cords (L1-3) were collected. The samples were embedded in paraffin, and 6-μm sections were prepared. Spinal cord tissue sections were immunostained with anti-ChAT antibody (Millipore) diluted 1:1,000 in Dako antibody diluent (Dako) using the EnVision+ System-HRP (Dako). ChAT-immunoreactive neurons in the ventral horn of the lumbar spinal cord (L1–3) were counted in 3 sections taken at 60-μm intervals, and the mean total number of ChAT-immunoreactive neurons was compared between treatment groups. The area (pixels) of ChAT-immunoreactive neurons was analyzed using NIH Image J software (NIH). ChAT-positive cells with an area greater than 100 μm^2 were presumed to be motor neurons.

NMJ assessment by immunohistochemical analysis

At the age of 120 days, 8 animals from each treatment group were sacrificed, and quadriceps femoris specimens were quickly frozen in liquid nitrogen. The samples were mounted in Tissue-Tek OCT compound (Sakura, Tokyo, Japan), and 30-μm cryostat sections were prepared from the frozen tissues. Frozen sections were fixed in acetone for 5 min and then incubated with TNB-buffer (0.10 M Tris-HCl, 0.15 M NaCl, 0.5% BMP) for 15 min at room temperature to block non-specific antibody binding. Sections were incubated with primary antibodies and alpha-BuTX overnight at 4°C. The following primary antibodies were used: anti-synaptophysin diluted 1:100 (Cell Signaling Technology) and anti-SMI31, 1:100 (COVANCE, Princeton, NJ, USA). Alpha-BuTX biotin-XX-conjugate diluted 1:80 was purchased from Molecular Probes (Eugene, OR, USA). After washing with PBS, the sections were exposed to appropriate secondary antibody and streptavidin-conjugated fluorescent dye for 1 h at room temperature, then washed with PBS again and mounted. Sections were examined and photographed using a confocal microscope (LSM 710, Carl Zeiss) under epifluorescent illumination.

Human sporadic ALS samples

Spinal cord specimens were obtained at autopsy from 3 pathologically confirmed cases of sALS (2 men, aged 71 and 73 y, and 1 woman, aged 53 y) and 3 cases of non-neurodegenerative disease. Lumbar spinal cord tissue was either homogenized for western blot analysis or embedded in paraffin for immunohistochemical analysis. The collection of autopsied human tissues and their use for this study were approved by the Ethics Committee of Nagoya University Graduate School of Medicine, and written informed consent was obtained from the patients' next-of-kin. Experimental procedures involving human subjects were conducted in conformance with the principles expressed in the Declaration of Helsinki.

Statistical analyses

Statistical analyses were performed using Prism software (GraphPad Software, La Jolla, CA, USA). Biochemical data were statistically analyzed using Student's t test or 1-factor factorial ANOVA followed by appropriate post-hoc tests. Survival data was analyzed by log-rank tests, and body weight change was analyzed by 2-factor factorial ANOVA. P values of 0.05 or less were considered to be statistically significant.

Supporting Information

Figure S1 Increased phosphorylated c-Abl in spinal cords of G93A mice. A: The distribution of phosphorylated c-Abl proteins was analyzed by immunohistochemical staining of paraffin-embedded spinal cord sections from G93A mice (10, 14, and 18 weeks old) and control littermates (20 weeks old) using antibodies directed against phosphorylated c-Abl (Tyr245 and Tyr412). The spinal sections were immunostained with anti-ChAT (red) and anti-phosphorylated c-Abl (Tyr245 or Tyr412) (green) antibodies together with Topro-3 (blue). Representative immunostained motor neurons visualized with confocal laser scanning microscopy are shown. Scale bar: 50 μm. B: The intensity of motor neurons labeled with anti-phosphorylated c-Abl (Tyr245) and anti-phosphorylated c-Abl (Tyr412) antibodies shown in A was quantified (n = 3 mice per group). Phosphorylated c-Abl immunoreactivity with both antibodies was significantly increased in the spinal cords of G93A mice ($P<0.01$). The value was standardized to that of the fluorescence intensity of control mice. Statistics were evaluated using 1-way ANOVA with Dunnett's post-hoc test. $^{**}P<0.01$.
(TIF)

Figure S2 Dasatinib reduced c-Abl phosphorylation (Tyr412) in G93A mice. A: Phosphorylated c-Abl (Tyr412) protein was analyzed by immunohistochemical staining of paraffin-embedded spinal cord sections from dasatinib-treated G93A mice (0, 5, 15, and 25 mg/(kg·day)) using an antibody against phosphorylated c-Abl (Tyr412). The spinal sections were fluorescently immunostained with anti-ChAT (red) and anti-phosphorylated c-Abl (Tyr412) (green) antibodies together with Topro-3 (blue). Representative immunostained motor neurons visualized with confocal laser scanning microscopy are shown. Scale bar: 50 μm. B: The intensity of the cells stained with anti-phosphorylated c-Abl (Tyr412) was quantified. The mice were administered the indicated amounts of dasatinib daily from postnatal day 56 to day 120 (n = 3 mice per group). Immunoreactivity against phosphorylated c-Abl (Tyr412) was significantly decreased in dasatinib-treated G93A mice (15 mg/(kg·day) or more) compared to vehicle-treated G93A mice ($P<0.01$, 15 mg/(kg·day) and 25 mg/(kg·day)). The value was standardized to that of the fluorescence intensity of vehicle-treated G93A mice. Statistics were evaluated using 1-way ANOVA with Dunnett's post-hoc test. $^{**}P<0.01$.
(TIF)

Acknowledgments

NSC-34 cells were kindly provided by Dr. N. Cashman. We thank Dr. E. Campeau for providing lentiviral expression systems.

Author Contributions

Conceived and designed the experiments: RK GS. Performed the experiments: RK SI MK KK JS. Analyzed the data: RK SI MK KK JS. Contributed reagents/materials/analysis tools: RK SI MK KK ZH JS HA FT FU. Wrote the paper: RK SI MK GS.

References

1. Tyler HR, Shefner J (1991) Amyotrophic lateral sclerosis. In: Vinken PJ, Bruyn GW, Klawans HL, editors. Handbook of Clinical Neurology. Amsterdam: Elsevier Science Publishers BV. pp. 169–215.
2. Emery A, Holloway S (1982) Familial motor neuron diseases. In: Rowland L, editor. Human Motor Neuron Diseases. New York: Raven Press Ltd. pp. 139–147.
3. Rosen DR, Siddique T, Patterson D, Figlewicz DA, Sapp P, et al. (1993) Mutations in Cu/Zn superoxide dismutase gene are associated with familial amyotrophic lateral sclerosis. Nature 362: 59–62.
4. Martin LJ, Liu Z, Chen K, Price AC, Pan Y, et al. (2007) Motor neuron degeneration in amyotrophic lateral sclerosis mutant superoxide dismutase-1 transgenic mice: mechanisms of mitochondriopathy and cell death. J Comp Neurol 500: 20–46.
5. Bruijn LI, Houseweart MK, Kato S, Anderson KL, Anderson SD, et al. (1998) Aggregation and motor neuron toxicity of an ALS-linked SOD1 mutant independent from wild-type SOD1. Science 281: 1851–1854.
6. Boillee S, Vande Velde C, Cleveland DW (2006) ALS: a disease of motor neurons and their nonneuronal neighbors. Neuron 52: 39–59.
7. Julien JP (2001) Amyotrophic lateral sclerosis. unfolding the toxicity of the misfolded. Cell 104: 581–591.
8. Kabashi E, Durham HD (2006) Failure of protein quality control in amyotrophic lateral sclerosis. Biochim Biophys Acta 1762: 1038–1050.
9. Cassina P, Cassina A, Pehar M, Castellanos R, Gandelman M, et al. (2008) Mitochondrial dysfunction in SOD1G93A-bearing astrocytes promotes motor neuron degeneration: prevention by mitochondrial-targeted antioxidants. J Neurosci 28: 4115–4122.
10. Jiang YM, Yamamoto M, Kobayashi Y, Yoshihara T, Liang Y, et al. (2005) Gene expression profile of spinal motor neurons in sporadic amyotrophic lateral sclerosis. Ann Neurol 57: 236–251.
11. Jiang YM, Yamamoto M, Tanaka F, Ishigaki S, Katsuno M, et al. (2007) Gene expressions specifically detected in motor neurons (dynactin 1, early growth response 3, acetyl-CoA transporter, death receptor 5, and cyclin C) differentially correlate to pathologic markers in sporadic amyotrophic lateral sclerosis. J Neuropathol Exp Neurol 66: 617–627.
12. Wang JY, Ledley F, Goff S, Lee R, Groner Y, et al. (1984) The mouse c-abl locus: molecular cloning and characterization. Cell 36: 349–356.
13. Nowell PC, Hungerford DA (1960) A minute chromosome in human chronic granulocytic leukemia. Science 132: 1488–1501.
14. Fainstein E, Marcelle C, Rosner A, Canaani E, Gale RP, et al. (1987) A new fused transcript in Philadelphia chromosome positive acute lymphocytic leukaemia. Nature 330: 386–388.
15. Brasher BB, Van Etten RA (2000) c-Abl has high intrinsic tyrosine kinase activity that is stimulated by mutation of the Src homology 3 domain and by autophosphorylation at two distinct regulatory tyrosines. J Biol Chem 275: 35631–35637.
16. Sirvent A, Benistant C, Roche S (2008) Cytoplasmic signalling by the c-Abl tyrosine kinase in normal and cancer cells. Biol Cell 100: 617–631.
17. Pendergast AM (2002) The Abl family kinases: mechanisms of regulation and signaling. Adv Cancer Res 85: 51–100.
18. Zandy NL, Playford M, Pendergast AM (2007) Abl tyrosine kinases regulate cell-cell adhesion through Rho GTPases. Proc Natl Acad Sci U S A 104: 17686–17691.
19. Gu JJ, Ryu JR, Pendergast AM (2009) Abl tyrosine kinases in T-cell signaling. Immunol Rev 228: 170–183.
20. Wang JY (2000) Regulation of cell death by the Abl tyrosine kinase. Oncogene 19: 5643–5650.
21. Yuan ZM, Shioya H, Ishiko T, Sun X, Gu J, et al. (1999) p73 is regulated by tyrosine kinase c-Abl in the apoptotic response to DNA damage. Nature 399: 814–817.
22. Wang JY, Ki SW (2001) Choosing between growth arrest and apoptosis through the retinoblastoma tumour suppressor protein, Abl and p73. Biochem Soc Trans 29: 666–673.
23. Lu W, Finnis S, Xiang C, Lee HK, Markowitz Y, et al. (2007) Tyrosine 311 is phosphorylated by c-Abl and promotes the apoptotic effect of PKCdelta in glioma cells. Biochem Biophys Res Commun 352: 431–436.
24. Chen TC, Lai YK, Yu CK, Juang JL (2007) Enterovirus 71 triggering of neuronal apoptosis through activation of Abl-Cdk5 signalling. Cell Microbiol 9: 2676–2688.
25. Lee JH, Jeong MW, Kim W, Choi YH, Kim KT (2008) Cooperative roles of c-Abl and Cdk5 in regulation of p53 in response to oxidative stress. J Biol Chem 283: 19826–19835.
26. Zukerberg LR, Patrick GN, Nikolic M, Humbert S, Wu CL, et al. (2000) Cables links Cdk5 and c-Abl and facilitates Cdk5 tyrosine phosphorylation, kinase upregulation, and neurite outgrowth. Neuron 26: 633–646.
27. Koleske AJ, Gifford AM, Scott ML, Nee M, Bronson RT, et al. (1998) Essential roles for the Abl and Arg tyrosine kinases in neurulation. Neuron 21: 1259–1272.
28. Cancino GI, Toledo EM, Leal NR, Hernandez DE, Yevenes LF, et al. (2008) STI571 prevents apoptosis, tau phosphorylation and behavioural impairments induced by Alzheimer's beta-amyloid deposits. Brain 131: 2425–2442.
29. Alvarez AR, Sandoval PC, Leal NR, Castro PU, Kosik KS (2004) Activation of the neuronal c-Abl tyrosine kinase by amyloid-beta-peptide and reactive oxygen species. Neurobiol Dis 17: 326–336.
30. Cashman NR, Durham HD, Blusztajn JK, Oda K, Tabira T, et al. (1992) Neuroblastoma x spinal cord (NSC) hybrid cell lines resemble developing motor neurons. Dev Dyn 194: 209–221.
31. Lombardo LJ, Lee FY, Chen P, Norris D, Barrish JC, et al. (2004) Discovery of N-(2-chloro-6-methyl- phenyl)-2-(6-(4-(2-hydroxyethyl)- piperazin-1-yl)-2-methylpyrimidin-4-ylamino)thiazole-5-carboxamide (BMS-354825), a dual Src/Abl kinase inhibitor with potent antitumor activity in preclinical assays. J Med Chem 47: 6658–6661.
32. Blake RA, Broome MA, Liu X, Wu J, Gishizky M, et al. (2000) SU6656, a selective src family kinase inhibitor, used to probe growth factor signaling. Mol Cell Biol 20: 9018–9027.
33. Alvarez AR, Klein A, Castro J, Cancino GI, Amigo J, et al. (2008) Imatinib therapy blocks cerebellar apoptosis and improves neurological symptoms in a mouse model of Niemann-Pick type C disease. FASEB J 22: 3617–3627.
34. Dangond F, Hwang D, Camelo S, Pasinelli P, Frosch MP, et al. (2004) Molecular signature of late-stage human ALS revealed by expression profiling of postmortem spinal cord gray matter. Physiol Genomics 16: 229–239.
35. Martin LJ (2010) Mitochondrial and cell death mechanisms in neurodegenerative diseases. Pharmaceuticals (Basel) 3: 839–915.
36. An X, Tiwari AK, Sun Y, Ding PR, Ashby CR, Jr., et al. (2010) BCR-ABL tyrosine kinase inhibitors in the treatment of Philadelphia chromosome positive chronic myeloid leukemia: a review. Leuk Res 34: 1255–1268.
37. Agrawal M, Garg RJ, Kantarjian H, Cortes J (2010) Chronic myeloid leukemia in the tyrosine kinase inhibitor era: what is the "best" therapy? Curr Oncol Rep 12: 302–313.
38. Braconi C, Bracci R, Cellerino R (2008) Molecular targets in Gastrointestinal Stromal Tumors (GIST) therapy. Curr Cancer Drug Targets 8: 359–366.
39. Isobe Y, Sugimoto K, Masuda A, Hamano Y, Oshimi K (2009) Central nervous system is a sanctuary site for chronic myelogenous leukaemia treated with imatinib mesylate. Intern Med J 39: 408–411.
40. Aichberger KJ, Herndlhofer S, Agis H, Sperr WR, Esterbauer H, et al. (2007) Liposomal cytarabine for treatment of myeloid central nervous system relapse in chronic myeloid leukaemia occurring during imatinib therapy. Eur J Clin Invest 37: 808–813.
41. Simpson E, O'Brien SG, Reilly JT (2006) Extramedullary blast crises in CML patients in complete hematological remission treated with imatinib mesylate. Clin Lab Haematol 28: 215–216.
42. Matsuda M, Morita Y, Shimada T, Miyatake J, Hirase C, et al. (2005) Extramedullary blast crisis derived from 2 different clones in the central nervous system and neck during complete cytogenetic remission of chronic myelogenous leukemia treated with imatinib mesylate. Int J Hematol 81: 307–309.
43. Rajappa S, Uppin SG, Raghunadharao D, Rao IS, Surath A (2004) Isolated central nervous system blast crisis in chronic myeloid leukemia. Hematol Oncol 22: 179–181.
44. Bujassoum S, Rifkind J, Lipton JH (2004) Isolated central nervous system relapse in lymphoid blast crisis chronic myeloid leukemia and acute lymphoblastic leukemia in patients on imatinib therapy. Leuk Lymphoma 45: 401–403.
45. Porkka K, Koskenvesa P, Lundan T, Rimpilainen J, Mustjoki S, et al. (2008) Dasatinib crosses the blood-brain barrier and is an efficient therapy for central nervous system Philadelphia chromosome-positive leukemia. Blood 112: 1005–1012.
46. Ito Y, Pandey P, Mishra N, Kumar S, Narula N, et al. (2001) Targeting of the c-Abl tyrosine kinase to mitochondria in endoplasmic reticulum stress-induced apoptosis. Mol Cell Biol 21: 6233–6242.
47. Gonfloni S (2010) DNA damage stress response in germ cells: role of c-Abl and clinical implications. Oncogene 29: 6193–6202.
48. Kanning KC, Kaplan A, Henderson CE (2010) Motor neuron diversity in development and disease. Annu Rev Neurosci 33: 409–440.
49. Vila M, Przedborski S (2003) Targeting programmed cell death in neurodegenerative diseases. Nat Rev Neurosci 4: 365–375.
50. Ludolph AC, Bendotti C, Blaugrund E, Hengerer B, Loffler JP, et al. (2007) Guidelines for the preclinical in vivo evaluation of pharmacological active drugs for ALS/MND: report on the 142nd ENMC international workshop. Amyotroph Lateral Scler 8: 217–223.
51. Inoue H, Tsukita K, Iwasato T, Suzuki Y, Tomioka M, et al. (2003) The crucial role of caspase-9 in the disease progression of a transgenic ALS mouse model. EMBO J 22: 6665–6674.
52. Campeau E, Ruhl VE, Rodier F, Smith CL, Rahmberg BL, et al. (2009) A versatile viral system for expression and depletion of proteins in mammalian cells. PLoS One 4: e6529.
53. Gurney ME, Pu H, Chiu AY, Dal Canto MC, Polchow CY, et al. (1994) Motor neuron degeneration in mice that express a human Cu,Zn superoxide dismutase mutation. Science 264: 1772–1775.
54. Adachi H, Kume A, Li M, Nakagomi Y, Niwa H, et al. (2001) Transgenic mice with an expanded CAG repeat controlled by the human AR promoter show polyglutamine nuclear inclusions and neuronal dysfunction without neuronal cell death. Hum Mol Genet 10: 1039–1048.

55. Adachi H, Waza M, Tokui K, Katsuno M, Minamiyama M, et al. (2007) CHIP overexpression reduces mutant androgen receptor protein and ameliorates phenotypes of the spinal and bulbar muscular atrophy transgenic mouse model. J Neurosci 27: 5115–5126.
56. Minamiyama M, Katsuno M, Adachi H, Waza M, Sang C, et al. (2004) Sodium butyrate ameliorates phenotypic expression in a transgenic mouse model of spinal and bulbar muscular atrophy. Hum Mol Genet 13: 1183–1192.
57. Katsuno M, Adachi H, Kume A, Li M, Nakagomi Y, et al. (2002) Testosterone reduction prevents phenotypic expression in a transgenic mouse model of spinal and bulbar muscular atrophy. Neuron 35: 843–854.
58. Ishigaki S, Liang Y, Yamamoto M, Niwa J, Ando Y, et al. (2002) X-Linked inhibitor of apoptosis protein is involved in mutant SOD1-mediated neuronal degeneration. J Neurochem 82: 576–584.

CROSS-SECTIONAL AND LONGITUDINAL ANALYSIS OF AN OXIDATIVE STRESS BIOMARKER FOR SPINAL AND BULBAR MUSCULAR ATROPHY

TOMOO MANO, MD,[1] MASAHISA KATSUNO, MD, PhD,[1] HARUHIKO BANNO, MD, PhD,[1,2] KEISUKE SUZUKI, MD, PhD,[1] NORIAKI SUGA, MD,[1] ATSUSHI HASHIZUME, MD, PhD,[1] FUMIAKI TANAKA, MD, PhD,[1] and GEN SOBUE, MD, PhD[1]

[1] Department of Neurology, Nagoya University Graduate School of Medicine, 65 Tsurumai-cho, Showa-ku, Nagoya 466-8550, Japan
[2] Institute for Advanced Research, Nagoya University, Nagoya, Japan

Accepted 6 April 2012

ABSTRACT: *Introduction:* Spinal and bulbar muscular atrophy (SBMA) is an adult-onset motor neuron disease caused by a CAG repeat expansion in the androgen receptor gene. The aim of this study was to verify whether urinary 8-hydroxydeoxyguanosine (8-OHdG), an oxidative stress marker, is a biomarker for SBMA. *Methods:* We measured the levels of urinary 8-OHdG in 33 genetically confirmed SBMA patients and 32 age-matched controls over a 24-month period at 6-month intervals. *Results:* Urinary 8-OHdG levels in SBMA patients were significantly elevated compared with those of controls and correlated well with motor function scores. During the follow-up period, urinary 8-OHdG levels increased and correlated with motor function at each time-point. In addition, urinary 8-OHdG levels at baseline were correlated with changes in the 6-minute walk test during 24 months. *Conclusions:* Urinary 8-OHdG is a biomarker for SBMA, reflecting the severity and possibly predicting the deterioration of motor function.

Muscle Nerve **46:** 692–697, 2012

Spinal and bulbar muscular atrophy (SBMA) is an hereditary, adult-onset, lower motor neuron disease. It is caused by aberrant elongation of a trinucleotide CAG repeat, which encodes a polyglutamine tract in the first exon of the androgen receptor (AR) gene.[1–3] The main symptoms are slowly progressive muscle weakness and atrophy of the bulbar, facial, and limb muscles. In general, the interval between the onset of weakness and death is 10–20 years.[4] An expanded CAG repeat has been identified as the cause of several neurodegenerative disorders, including SBMA, Huntington disease (HD), and several forms of spinocerebellar ataxia.[5] Although the causative genes show little homology other than the presence of a CAG repeat, these polyglutamine-mediated disorders share common pathways of molecular pathogenesis, such as transcriptional dysregulation, axonal transport defects, and mitochondrial dysfunction.[6,7]

Although animal studies have indicated the beneficial effects of androgen deprivation for SBMA, the results of clinical trials were inconclusive.[8–10] This is likely attributable to the difficulties in evaluating the disease-modifying effects of the tested drugs due to the slow progression of the neurological symptoms in SBMA. Therefore, appropriate surrogate endpoints are needed to facilitate the proof-of-concept of potential therapies for this disease. In this regard, it is important to identify biomarkers for SBMA that reflect the pathogenic processes and can be used as indicators of therapeutic efficacy. Although the nuclear accumulation of mutant AR protein in the scrotal skin has been shown to be a candidate histopathological biomarker, its practical use is limited due to the invasive nature of the procedure.[11,12] Conversely, non-invasive serum or urinary markers to evaluate disease severity have not been established for SBMA.

Oxidative stress resulting from mitochondrial dysfunction has been implicated in aging and neurodegeneration.[13] Pathogenic huntingtin, the causative protein of HD, induces oxidative stress through its direct association with mitochondria and downregulation of mitochondrial transcriptional regulators.[14,15] In a cellular model of SBMA, the expression of pathogenic AR is associated with depolarization of the mitochondrial membrane and an increase in the levels of reactive oxygen species (ROS), which is attenuated by the antioxidants coenzyme Q10 and idebenone.[16] ROS, such as hydroxyl radicals and H_2O_2, react with guanine residues in DNA and produce 8-hydroxydeoxyguanosine (8-OHdG), which is excreted in the urine, thereby serving as a biomarker of oxidative DNA damage.[17]

The aim of this study was to evaluate the validity of urinary 8-OHdG as a biomarker for SBMA. In particular, we investigated whether the urinary levels of 8-OHdG reflect the disease severity of SBMA patients. We also investigated the natural history of this parameter in order to determine whether it can be used to monitor disease progression.

METHODS

Participants. We studied 33 patients with SBMA and 32 age-matched, normal controls (Table 1). The inclusion criteria were: a clinical diagnosis of

Abbreviations: 6MWT, 6-minute walk test; 8-OHdG, 8-hydroxydeoxyguanosine; ALS, amyotrophic lateral sclerosis; ALSFRS-R, ALS Functional Rating Scale-revised; AR, androgen receptor; BMI, body mass index; HbA_{1c}, glycated hemoglobin; HD, Huntington disease; LNS, limb Norris score; NBS, Norris bulbar score; PCR, polymerase chain reaction; ROS, reactive oxygen species; SBMA, spinal and bulbar muscular atrophy

Key words: androgen receptor, biomarker, motor neuron, oxidative stress, spinal and bulbar muscular atrophy

Correspondence to: M. Katsuno; e-mail: ka2no@med.nagoya-u.ac.jp or G. Sobue; e-mail: sobueg@med.nagoya-u.ac.jp

© 2012 Wiley Periodicals, Inc.

Published online 31 August 2012 in Wiley Online Library (wileyonlinelibrary.com). DOI 10.1002/mus.23413

Table 1. Clinical and genetic features of the SBMA patients and controls.

Clinical and genetic features	SBMA	Control	*P*-value
Number of subjects	33	32	
Age at examination (years)	54.7 ± 10.1 (27–72)	52.8 ± 12.8 (36–74)	0.879
BMI*	22.8 ± 3.4 (15.1–27.6)	25.0 ± 6.7 (17.9–29.0)	0.465
CAG repeat length in AR gene	48.4 ± 3.9 (40–57)		
Duration from onset (years)	10.0 ± 6.8 (2–22)		
Hypertension	11 (34.4%)	12 (36.4%)	0.099
Hyperlipidemia	5 (15.6%)	7 (21.2%)	0.299
Diabetes	2 (6.3%)	3 (9.1%)	0.509
HbA_{1c} (%)	5.3 ± 0.5 (4.3–7.2)	5.3 ± 0.4 (4.8–6.1)	0.953

Data are shown as number, mean ± SD (range), or number (%). BMI, body mass index; AR, androgen receptor; HbA_{1c}, glycated hemoglobin.

SBMA with more than 1 motor symptom (i.e., muscle weakness, muscle atrophy, bulbar palsy, and hand tremor) and confirmation by genetic analysis; age between 25 and 75 years; and the ability to walk with or without a cane. We evaluated disease severity using the clinical scales for amyotrophic lateral sclerosis (ALS), such as the limb Norris score (LNS), the Norris bulbar score (NBS), and the ALS Functional Rating Scale-revised; (ALSFRS-R) score. We also measured motor function using clinical tests such as the 6-minute walk test (6MWT) and grip power.[18,19] We defined the onset of disease as the time when muscle weakness began, but not when tremor of the fingers appeared. The first examination was performed between June and November 2008. All patients were outpatients. In this longitudinal study, the SBMA patients were followed for 24 months at 6-month intervals. During follow-up, 3 patients did not complete the assessment due to difficulty in visiting the hospital regularly. This study conformed to the ethics guidelines for human genome/gene analysis research and epidemiological studies endorsed by the Japanese government. The institutional review board of the Nagoya University Graduate School of Medicine approved the study, and all SBMA patients and normal subjects gave informed consent for participation in the investigation.

Urinary 8-OHdG. Urine samples were obtained from each individual in the morning (9:00 a.m. to 12:00 noon) and were immediately stored at −20°C. Age-matched controls were selected from male examinees undergoing health check-ups between March and April 2009, at the Chuo Clinic, Nagoya. We included control subjects with ages between 25 and 75 years, and those who had any neurological symptoms or findings were excluded. We instructed the patients and controls to avoid strenuous exercise in the 24 h before providing the sample, because it was shown that exercise increases the urinary levels of 8-OHdG.[20,21] All samples from the same time-point were measured simultaneously. We de-identified the samples, and the urinary levels of 8-OHdG and creatinine were anonymously measured using an enzyme-linked immunosorbent assay (ELISA) with a specific monoclonal antibody (N45.1; Japan Institute for the Control of Aging, Furoi, Japan) at Mitsubishi Chemical Medicine Co. (Tokyo, Japan).[22] The urinary levels of 8-OHdG were normalized in relation to creatinine levels to adjust for the urine volume.

Genetic Analysis. Genomic DNA was extracted from the peripheral blood of SBMA patients using conventional techniques. Polymerase chain reaction (PCR) amplification of the CAG repeat in the AR gene was performed using a fluorescein-labeled forward primer (5′-TCCAGAATCTGTTCCAGAGCG TGC-3′) and an unlabeled reverse primer (5′-TGG CCTCGCTCAGGATGTCTTTAAG-3′). The detailed PCR conditions and measurement of the CAG-repeat size have been described elsewhere.[23]

Data Analysis. All data are presented as mean ± SD. Patient–control differences in categorical variables were assessed using the chi-square test. Longitudinal changes in the parameters were compared using a paired *t*-test, where the null hypothesis was that there was no change between baseline and the end of the 24-month follow-up. Correlations among the parameters were analyzed using Pearson correlation coefficients. We used multiple regression analysis for multiple classification analysis. $P < 0.05$ and correlation coefficients (r) > 0.4 were considered significant. Calculations were performed using SPSS version 14.0J (SPSS Japan, Tokyo, Japan) statistical software.

RESULTS

Clinical Backgrounds and Urinary 8-OHdG Levels in the SBMA Patients. The clinical characteristics of the study population are listed in Table 1. There were a total of 33 SBMA patients in the study. All participants were male and of Japanese nationality. There was no substantial difference between the median CAG repeat length in the SBMA population enrolled in this study and those reported previously.[4,9,24] Two of the 33 patients needed a cane

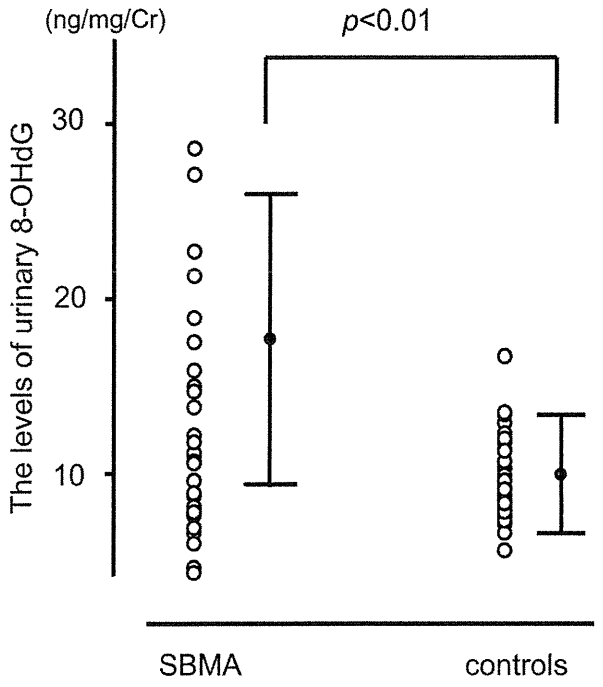

FIGURE 1. Urinary levels of 8-OHdG in SBMA patients and controls. Levels of urinary 8-OHdG in 33 SBMA patients were significantly higher than in the 32 age-matched controls ($P < 0.01$).

for ambulation. None were bedridden or wheelchair-bound. The prevalence of hypertension, hyperlipidemia, and diabetes mellitus as well as the value of glycated hemoglobin (HbA_{1c}) were equivalent between the SBMA patients and controls. Levels of urinary 8-OHdG in the SBMA patients (11.8 ± 6.2 ng/mg) were significantly higher than in the controls (9.7 ± 2.5 ng/mg) ($P < 0.01$) (Fig. 1). Two patients with especially high levels of urinary 8-OHdG (28.6 and 27.1 ng/mg) were at an advanced age (58 and 60 years, respectively) and had diabetes mellitus.

Correlation between Urinary 8-OHdG and Clinical Severity. The urinary 8-OHdG levels correlated well with all clinical scales and measures of motor function, namely ALSFRS-R, 6MWT, LNS, NBS, and grip power (Fig. 2 and Table 2). There was no correlation between urinary 8-OHdG levels and body mass index (BMI). Although age at examination was correlated with urinary 8-OHdG levels in the SBMA patients ($r = -0.401$), this relationship was not observed in the controls ($r = -0.124$). No relationship was found between the urinary 8-OHdG levels and the age at onset, the number of

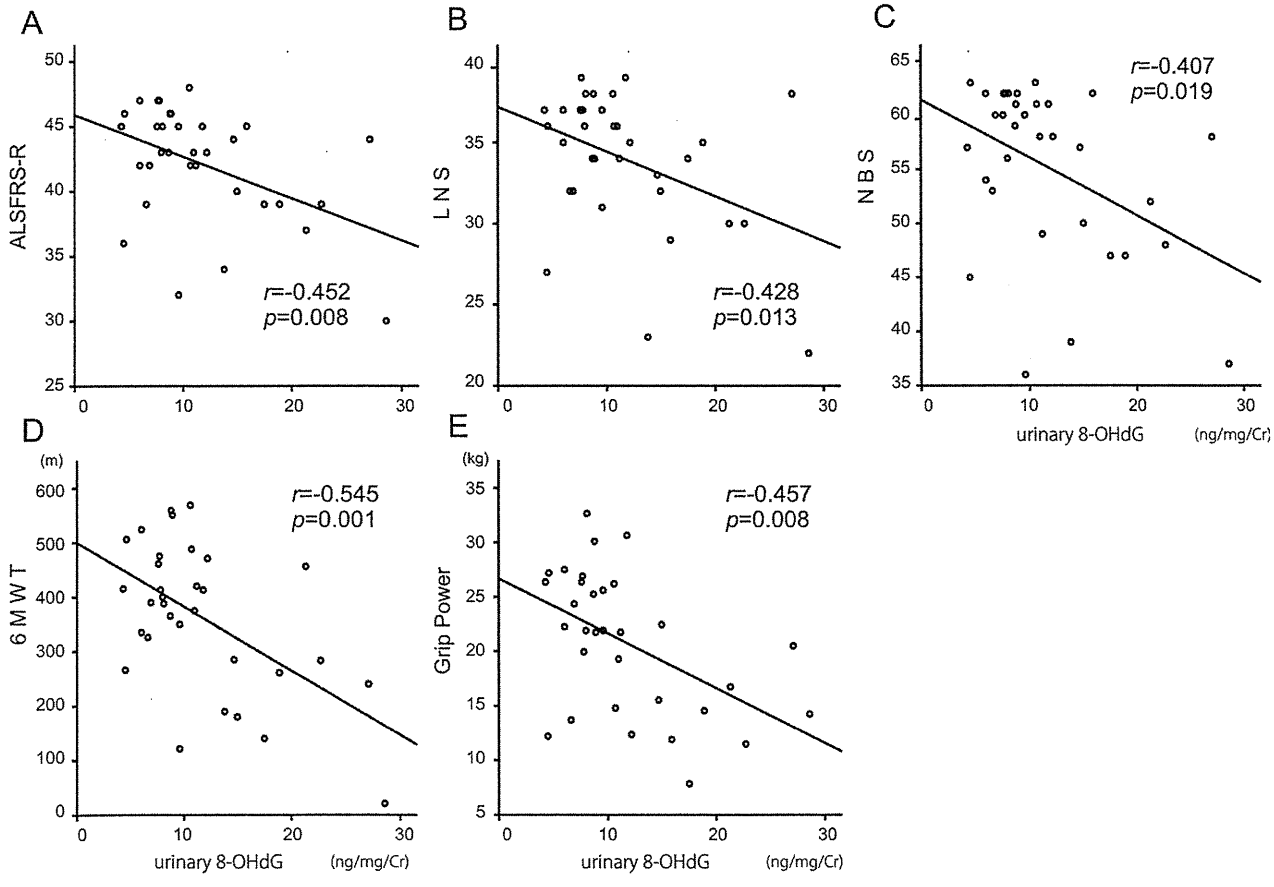

FIGURE 2. Correlation between levels of urinary 8-OHdG and motor function parameters. **(A–C)** Urinary 8-OHdG levels correlated with the scores of motor function scales, including the ALS Functional Rating Scale-revised; (ALSFRS-R) **(A)**, limb Norris score (LNS) **(B)**, and Norris bulbar score (NBS) **(C)** in the SBMA patients. **(D–E)** Similarly, there was a correlation between the levels of urinary 8-OHdG and the results of motor function tests, such as the 6-minute walk test (6MWT) **(D)** and grip power **(E)**.

Table 2. Correlation of urinary 8-OHdG and other clinical parameters in SBMA patients at baseline ($n = 33$).

	Measured value	Correlation with urinary 8-OHdG	*P*-value
ALSFRS-R	42.1 ± 4.4	$r = -0.452$	0.008
LNS	55.2 ± 7.8	$r = -0.428$	0.013
NBS	34.0 ± 4.2	$r = -0.407$	0.019
6MWT (m)	363.7 ± 135.9	$r = -0.545$	0.001
Grip power (kg)*	20.2 ± 7.3	$r = -0.457$	0.008
Age at examination (years)	54.7 ± 10.1	$r = -0.401$	0.021
Number of CAG repeats	48.4 ± 3.9	$r = -0.221$	0.223
Duration from onset (years)	10.0 ± 6.8	$r = -0.03$	0.891
Age at onset (years)	42.2 ± 12.4	$r = -0.271$	0.186
BMI	22.8 ± 3.4	$r = 0.186$	0.326
HbA_{1c} (%)	5.3 ± 0.5	$r = 0.309$	0.080

Data are presented as mean ± SD. ALSFRS-R, ALS Functional Rating Scale-revised; (normal score = 48); LNS, limb Norris score (normal score = 63); NBS, Norris bulbar score (normal score = 39); 6MWT, 6-minute walk test.
**Average of both hands.*

CAG repeats, or disease duration in the SBMA patients. In multiple regression analysis, clinical tests of general motor function, such as grip power and 6MWT, correlated with the urinary levels of 8-OHdG (grip power, $r = -0.512$; 6MWT, $r = -0.442$). There was no detectable correlation between urinary 8-OHdG levels and the other parameters, including HbA_{1c}.

Longitudinal Analysis of Urinary 8-OHdG levels in the SBMA Patients. Due to the withdrawal of 3 patients, we analyzed the remaining 30 patients in the longitudinal study. Urinary 8-OHdG levels showed a significant increase during the 24-month follow-up period ($P < 0.05$) (Table 3). The other clinical scales and measures of motor function also showed a significant increase during this period ($P < 0.05$) (Table 3). During the follow-up period, urinary 8-OHdG levels increased and were correlated with each measure of motor function at all time-points examined (Table 4). Next, we investigated whether the change in the levels of urinary 8-OHdG reflects the degree of disease progression. The percentage of change from baseline was used to analyze each parameter. The levels of urinary 8-OHdG at baseline correlated with the changes of 6MWT during 24 months, suggesting that the intensity of oxidative stress at baseline is associated with the prognosis for ambulatory capacity (Table 5). There was, however, no correlation between the change in urinary 8-OHdG levels and that of the clinical scores or measures (Table 5).

DISCUSSION

This study has shown that urinary 8-OHdG levels are significantly increased in patients with SBMA compared with controls. Moreover, the urinary 8-OHdG levels in SBMA patients correlated with the motor function scores in our cross-sectional study. Our results thus show that urinary 8-OHdG, an oxidative stress marker, is a biomarker that reflects disease severity in patients with SBMA. 8-OHdG is produced by the reaction between ROS and guanine residues in DNA. The ROS-mediated formation of mutated mtDNA has been implicated in the pathogenesis of age-related disorders such as neurodegenerative disorders, type II diabetes, cancer, and cardiac diseases.[25] Generally, the levels of urinary 8-OHdG are not strongly elevated by aging.[26] Our results, however, show that the urinary 8-OHdG levels correlated with age in SBMA patients. Given the strong correlation between the urinary 8-OHdG levels and the motor function scores, this may be due to the fact that the condition of aged SBMA patients is more severe than that of younger patients. In support of this view, multiple regression analysis showed that the urinary levels of 8-OHdG were correlated with motor function parameters, but not with the age of SBMA patients. Diabetes mellitus, a putative trigger of oxidative stress,[27] was found in the 2 SBMA patients who had elevated levels of urinary 8-OHdG. Nevertheless, there was no strong correlation between the levels of urinary 8-OHdG and HbA_{1c} levels.

Increased oxidative stress has been detected in various diseases, including neurological disorders.

Table 3. Changes in urinary 8-OHdG and other parameters in SBMA patients during 24-month follow-up ($n = 30$).

	0 month ($n = 30$)	6 months ($n = 30$)	12 months ($n = 30$)	18 months ($n = 30$)	24 months ($n = 30$)	Change in 24 months
Urinary 8-OHdG (ng/mg/Cr)	11.6 ± 6.5	16.9 ± 7.8	16.5 ± 7.8	18.8 ± 8.1	17.5 ± 7.9	6.0 ± 5.1*
ALSFRS-R	42.2 ± 4.2	42.4 ± 4.0	41.8 ± 4.0	41.0 ± 3.9	40.7 ± 3.8	−1.5 ± 1.9*
LNS	56.0 ± 6.9	56.0 ± 6.6	54.1 ± 7.7	52.9 ± 7.9	51.8 ± 7.8	−3.5 ± 3.9*
NBS	33.6 ± 4.4	33.9 ± 4.1	33.4 ± 4.3	33.0 ± 4.9	32.4 ± 4.6	−2.0 ± 2.4*
6MWT (m)	367.8 ± 136.4	357.8 ± 137.9	348.8 ± 142.3	337.7 ± 138.3	331.7 ± 132.3	−36.1 ± 2.5*
Grip power (kg)	21.0 ± 6.6	20.7 ± 6.6	20.2 ± 6.4	18.9 ± 7.2	18.9 ± 7.1	−1.9 ± 2.9†

Data are presented as mean ± SD. ALSFRS-R, ALS Functional Rating Scale-revised; LBS, limb Norris score; NBS, Norris bulbar score; 6MWT, 6-minute walk test.
**$P < 0.001$ for comparison between 0 month and 24 months (paired t-test).*
†$P = 0.001$ for comparison between 0 month and 24 months (paired t-test).

Table 4. Correlations between urinary 8-OHdG and other parameters in SBMA patients during 24-month follow-up.

	Correlation with urinary 8-OHdG			
	6 months ($n = 30$)	12 months ($n = 30$)	18 months ($n = 30$)	24 months ($n = 30$)
ALSFRS-R	$r = -0.454$	$r = -0.472$	$r = -0.586$	$r = -0.665$
	$P = 0.012$	$P = 0.008$	$P = 0.001$	$P < 0.001$
LNS	$r = -0.482$	$r = -0.408$	$r = -0.550$	$r = -0.610$
	$P = 0.007$	$P = 0.025$	$P = 0.002$	$P < 0.001$
NBS	$r = -0.390$	$r = -0.531$	$r = -0.550$	$r = -0.593$
	$P = 0.033$	$P = 0.003$	$P = 0.002$	$P = 0.001$
6MWT (m)	$r = -0.457$	$r = -0.372$	$r = -0.552$	$r = -0.542$
	$P = 0.011$	$P = 0.043$	$P = 0.002$	$P = 0.002$
Grip power (kg)	$r = -0.605$	$r = -0.409$	$r = -0.457$	$r = -0.508$
	$P < 0.001$	$P = 0.025$	$P = 0.011$	$P = 0.004$

ALSFRS-R, ALS Functional Rating Scale-revised; LNS, limb Norris score; NBS, Norris bulbar score; 6MWT, 6-minute walk test.

Recent studies have suggested that oxidative stress appears be a common process in a number of neurodegenerative diseases, such as ALS, Alzheimer disease, Parkinson disease, and HD.[28–32] The association between neurodegeneration and oxidative stress has been best described in Parkinson disease, autosomal recessive forms of which are caused by mutations in the genes *Parkin*, *DJ1*, and PTEN-induced putative kinase1 (*PINK1*), which play a role in the degradation of abnormal mitochondria via autophagy.[33] Patients with polyglutamine diseases, including SBMA, have a relatively low mitochondrial DNA copy number in leukocytes, which is inversely correlated with the length of the CAG repeat in causative genes.[34,35] Abnormal mitochondria have been detected in a knock-in mouse model of SBMA.[16] The amino-terminal fragment of polyglutamine-expanded AR induces mitochondrial damage through the activation of c-Jun N-terminal kinase.[36] Pathogenic AR also reduces the mRNA levels of peroxisome proliferator–activated receptor γ coactivator-1beta (PGC-1β) as well as those of various antioxidant genes in cellular and animal models of SBMA.[16] The increased levels of 8-OHdG in our study confirm the implication of oxidative stress in SBMA.

Urinary 8-OHdG is considered to be a reliable biomarker of oxidative stress, because the excised 8-OHdG is excreted in the urine without compensation by anti-oxidative agents in the plasma. Thus, the measure of urinary 8-OHdG has gained attention as a biomarker of neurodegenerative disease. The urinary levels of 8-OHdG were shown to be correlated with disease severity in Parkinson disease and ALS.[37,38] In this study, the urinary levels of 8-OHdG correlated significantly with the scores of motor function and other functional parameters at all timepoints, suggesting that this parameter appears to be a biomarker that reflects the severity of SBMA.

There have been a limited number of studies on the chronological changes in oxidative stress markers in neurodegenerative diseases.[29] In our longitudinal analysis, we confirmed the significant increase in urinary levels of 8-OHdG, suggesting the accumulation of oxidative stress in SBMA patients during the observation period. Furthermore, levels of urinary 8-OHdG at baseline correlated with changes in the 6MWT during the 24 months of observation, indicating that increased oxidative stress is associated with a poor prognosis for ambulatory function in SBMA patients. In support of this view, chemical induction of oxidative stress was shown to exacerbate neurodegeneration in rodents.[39] However, baseline levels of urinary 8-OHdG did not correlate with changes of other functional measures over the 24 months of the present study. Neither were the changes of urinary 8-OHdG levels paralleled by those of the motor function parameters. This discrepancy may result from intrasubject fluctuations of the functional scores or the relatively short observation period of the study. Alternatively, the fact that the functional scales, but not the 6MWT, are vulnerable to patient and rater subjectivity may mask the correlation between levels of urinary 8-OHdG and changes in motor function scores.[40]

Validated biomarkers are key to the development of disease-modifying therapies for neurodegenerative disorders.[41] Although a number of candidate therapeutics have emerged from basic studies, most have failed to show positive results in clinical trials for neurodegenerative diseases. A lack of sensitive and reliable measures of pharmacological effects is one of the factors preventing successful translation of animal studies to the clinic. The use of biomarkers in exploratory-phase clinical trials may facilitate the selection of agents for further testing in confirmatory-phase trials and

Table 5. Correlation between changes in urinary 8-OHdG and other parameters ($n = 30$).

	8-OHdG (0 month)	Δ8-OHdG (0–6 months)	Δ8-OHdG (0–24 months)
ΔALSFRS-R*	$r = -0.70$	$r = 0.167$	$r = 0.173$
	($P = 0.713$)	($P = 0.379$)	($P = 0.389$)
ΔLNB*	$r = -0.288$	$r = 0.051$	$r = 0.081$
	($P = 0.123$)	($P = 0.787$)	($P = 0.671$)
ΔNBS*	$r = -0.113$	$r = 0.041$	$r = 0.032$
	($P = 0.551$)	($P = 0.830$)	($P = 0.865$)
Δ6MWT*	$r = -0.376$	$r = 0.102$	$r = 0.037$
	($P = 0.040$)	($P = 0.591$)	($P = 0.847$)
ΔGrip power*	$r = -0.050$	$r = -0.107$	$r = -0.108$
	($P = 0.793$)	($P = 0.575$)	($P = 0.570$)

ALSFRS-R, ALS Functional Rating Scale-revised; LNS, limb Norris score; NBS, Norris bulbar score; 6MWT, 6-minute walk test.
**Changes between 0 and 24 months.*

the stratification of those patients who will be most likely to benefit from the therapy.[42] The urinary levels of 8-OHdG have been used as an endpoint in clinical trials for neurological disorders.[29,43,44] Given that several drugs have been developed for SBMA, the plausibility of urinary 8-OHdG as a biomarker should also be examined in clinical trials.

This work was supported by a Center of Excellence (COE) grant, a Grant-in-Aid for Scientific Research on Innovative Areas "Foundation of Synapse and Neurocircuit Pathology," and Grants-in-Aid from Ministry of Education, Culture, Sports, Science, and Technology of Japan; grants from the Ministry of Health, Labor and Welfare of Japan; and Core Research for Evolutional Science and Technology (CREST) from the Japan Science and Technology Agency (JST).

REFERENCES

1. Kennedy WR, Alter M, Sung JH. Progressive proximal spinal and bulbar muscular atrophy of late onset: a sex-linked recessive trait, Neurology 1968;18:671–680.
2. Sperfeld AD, Karitzky J, Brummer D, Schreiber H, Häussler J, Ludolph AC, et al. X-linked bulbospinal neuronopathy: Kennedy disease. Arch Neurol 2002;59:1921–1926.
3. Fischbeck KH. Kennedy disease. J Inherit Metab Dis 1997;20: 152–158.
4. Atsuta N, Watanabe H, Ito M, Banno H, Suzuki K, Katsuno M, et al. Natural history of spinal and bulbar muscular atrophy (SBMA): a study of 223 Japanese patients. Brain 2006;129:1446–1455.
5. Andrew SE, Goldberg YP, Hayden MR. Rethinking genotype and phenotype correlations in polyglutamine expansion disorders. Hum Mol Genet 1997;6:2005–2010.
6. La Spada AR, Taylor JP. Repeat expansion disease: progress and puzzles in disease pathogenesis. Nat Rev Genet 2010;11:247–258.
7. Katsuno M, Adachi H, Waza M, Banno H, Suzuki K, Tanaka F, et al. Pathogenesis, animal models and therapeutics in spinal and bulbar muscular atrophy (SBMA). Exp Neurol 2006;200:8–18.
8. Katsuno M, Adachi H, Doyu M, Minamiyama M, Sang C, Kobayashi T, et al. Leuprorelin rescues polyglutamine-dependent phenotypes in a transgenic mouse model of spinal and bulbar muscular atrophy. Nat Med 2003;9:768–773.
9. Katsuno M, Banno H, Suzuki K, Takeuchi Y, Kawashima M, Yabe I, et al. Efficacy and safety of leuprorelin in patients with spinal and bulbar muscular atrophy (JASMITT study): a multicentre, randomised, double-blind, placebo-controlled trial. Lancet Neurol 2010;9: 875–884.
10. Fernández-Rhodes LE, Kokkinis AD, White MJ, Watts CA, Auh S, Jeffries NO, et al. Efficacy and safety of dutasteride in patients with spinal and bulbar muscular atrophy: a randomised placebo-controlled trial. Lancet Neurol 2011;10:140–147.
11. Banno H, Adachi H, Katsuno M, Suzuki K, Astuta N, Watanabe H, et al. Mutant androgen receptor accumulation in spinal and bulbar muscular atrophy scrotal skin: a pathogenic marker. Ann Neurol 2006;59:520–526.
12. Suzuki K, Katsuno M, Banno H, Takeuchi Y, Kawashima M, Suga N, et al. The profile of motor unit number estimation (MUNE) in spinal and bulbar muscular atrophy. J Neurol Neurosurg Psychiatry 2010;81:567–571.
13. Martin LJ. DNA damage and repair: relevance to mechanisms of neurodegeneration. J Neuropathol Exp Neurol 2008;67:377–387.
14. Cui L, Jeong H, Borovecki F, Parkhurst CN, Tanese N, Krainc D. Transcriptional repression of PGC-1alpha by mutant huntingtin leads to mitochondrial dysfunction and neurodegeneration. Cell 2006;127:59–69.
15. Browne SE. Mitochondria and Huntington's disease pathogenesis: insight from genetic and chemical models. Ann NY Acad Sci 2008; 1147:358–382.
16. Ranganathan S, Harmison GG, Meyertholen K, Pennuto M, Burnett BG, Fischbeck KH. Mitochondrial abnormalities in spinal and bulbar muscular atrophy. Hum Mol Genet 2009;18:27–42.
17. Alam ZI, Jenner A, Daniel SE, Lees AJ, Cairns N, Marsden CD, et al. Oxidative DNA damage in the parkinsonian brain: an apparent selective increase in 8-hydroxyguanine levels in substantia nigra. J Neurochem 1997;69:1196–1203.
18. ATS Committee on Proficiency Standards for Clinical Pulmonary Function Laboratories. ATS statement: Guidelines for the six-minute walk test. Am J Respir Crit Care Med 2002;166:111–117.
19. Takeuchi Y, Katsuno M, Banno H, Suzuki K, Kawashima M, Atsuta N, et al. Walking capacity evaluated by the 6-minute walk test in spinal and bulbar muscular atrophy. Muscle Nerve 2008;38:964–971.
20. Morillas-Ruiz J, Zafrilla P, Almar M, Cuevas MJ, López FJ, Abellán P, et al. The effects of an antioxidant-supplemented beverage on exercise-induced oxidative stress: results from a placebo-controlled double-blind study in cyclists. Eur J Appl Physiol 2005;95:543–549.
21. Muñoz ME, Galan AI, Palacios E, Diez MA, Muguerza B, Cobaleda C, et al. Effect of an antioxidant functional food beverage on exercise-induced oxidative stress: a long-term and large-scale clinical intervention study. Toxicology 2010;28:101–111.
22. Saito S, Yamauchi H, Hasui Y, Kurashige J, Ochi H, Yoshida K. Quantitative determination of urinary 8-hydroxydeoxyguanosine (8-OH-dg) by using ELISA. Res Commun Mol Pathol Pharmacol 2000;107:39–44.
23. Doyu M, Sobue G, Mukai E, Kachi T, Yasuda T, Mitsuma T, et al. Severity of X-linked recessive bulbospinal neuronopathy correlates with size of the tandem CAG repeat in androgen receptor gene. Ann Neurol 1992;32:707–710.
24. Dejager S, Bry-Gauillard H, Bruckert E, Eymard B, Salachas F, LeGuern E, et al. A comprehensive endocrine description of Kennedy's disease revealing androgen insensitivity linked to CAG repeat length. J Clin Endocrinol Metab 2002;87:3893–3901.
25. Nakanishi S, Suzuki G, Kusunoki Y, Yamane K, Egusa G, Kohno N. Increasing of oxidative stress from mitochondria in type 2 diabetic patients. Diabetes Metab Res Rev 2004;20:399–404.
26. Kimura S, Yamauchi H, Hibino Y, Iwamoto M, Sera K, Ogino K. Evaluation of urinary 8-hydroxydeoxyguanine in healthy Japanese people. Basic Clin Pharmacol Toxicol 2006;98:496–502.
27. Yu P, Wang Z, Sun X, Chen X, Zeng S, Chen L, et al. Hydrogen-rich medium protects human skin fibroblasts from high glucose or mannitol induced oxidative damage. Biochem Biophys Res Commun 2011;409:350–355.
28. Montine TJ, Beal MF, Cudkowicz ME, O'Donnell H, Margolin RA, McFarland L, et al. Increased CSF F2-isoprostane concentration in probable AD. Neurology 1999;52:562–565.
29. Hersch SM, Gevorkian S, Marder K, Moskowitz C, Feigin A, Cox M, et al. Creatine in Huntington's disease is safe, tolerable, bioavailable in brain and reduces serum 8OH2′dG. Neurology 2006;66:250–252.
30. Casadesus G, Smith MA, Basu S, Hua J, Capobianco DE, Siedlak SL, et al. Increased isoprostane and prostaglandin are prominent in neurons in Alzheimer's disease. Mol Neurodegen 2007;2:2.
31. Kikuchi A, Takeda A, Onodera H, Kimpara T, Hisanaga K, Sato N, et al. Systemic increase of oxidative nucleic acid damage in Parkinson's disease and multiple system atrophy. Neurobiol Dis 2002;9:244–248.
32. Hirayama M, Nakamura T, Watanabe H, Uchida K, Hama T, Hara T, et al. Parkinsonism Relat Disord 2011;17:46–49.
33. Meissner WG, Frasier M, Gasser T, Goetz CG, Lozano A, Piccini P, et al. Priorities in Parkinson's disease research. Nat Rev Drug Discov 2011;10:377–393.
34. Liu Y, Prasad R, Beard WA, Hou EW, Horton JK, McMurray CT, et al. Coordination between polymerase beta and FEN1 can modulate CAG repeat expansion. J Biol Chem 2009;284:28352–28366.
35. Su S, Jou S, Cheng W, Lin T, Li J, Huang C, et al. Mitochondrial DNA damage in spinal and bulbar muscular atrophy patients and carriers. Clin Chim Acta 2010;411:626–630.
36. Young JE, Garden GA, Martinez RA, Tanaka F, Sandoval CM, Smith AC, et al. Polyglutamine-expanded androgen receptor truncation fragments activate a Bax-dependent apoptotic cascade mediated by DP5/Hrk. J Neurosci 2009;18:1987–1997.
37. Sato S, Mizuno Y, Hattori N. Urinary 8-hydroxydeoxyguanosine levels as a biomarker for progression of Parkinson disease. Neurology 2005;64:1081–1083.
38. Mitsumoto H, Santella RM, Liu X, Bogdanov M, Zipprich J, Wu HC, et al. Oxidative stress biomarkers in sporadic ALS. Amyotroph Lateral Scler 2008;9:177–183.
39. Tong L, Wan M, Zhou D, Gao J, Zhu Y, Bi K. LC-MS/MS determination and pharmacokinetic study of albiflorin and paeoniflorin in rat plasma after oral administration of Radix Paeoniae Alba extract and Tang-Min-Ling-Wan. Biomed Chromatogr 2010;24:1324–1331.
40. Hashizume A, Katsuno M, Banno H, Suzuki K, Suga N, Tanaka F, et al. Difference in chronological changes of outcome measures between untreated and placebo-treated patients of spinal and bulbar muscular atrophy. J Neurol 2012;259:712–719.
41. Katsuno M, Tanaka F, Sobue G. Perspectives on molecular targeted therapies and clinical trials for neurodegenerative diseases J Neurol Neurosurg Psychiatry 2012;83:329–335.
42. Hampel H, Frank R, Broich K, Teipel SJ, Katz RG, Hardy J, et al. Biomarkers for Alzheimer's disease: academic, industry and regulatory perspectives. Nat Rev Drug Discov 2010;9:560–574.
43. Di Prospero NA, Baker A, Jeffries N, Fischbeck KH. Neurological effects of high-dose idebenone in patients with Friedreich's ataxia: a randomised, placebo-controlled trial. Lancet Neurol 2007;6:878–886.
44. Boesch S, Sturm B, Hering S, Scheiber-Mojdehkar B, Steinkellner H, Goldenberg H, et al. Neurological effects of recombinant human erythropoietin in Friedreich's ataxia: a clinical pilot trial. Mov Disord 2008;23:1940–1944.

doi:10.1093/brain/aws170 Brain 2012: 135; 2838–2848 | 2838

BRAIN
A JOURNAL OF NEUROLOGY

Longitudinal changes of outcome measures in spinal and bulbar muscular atrophy

Atsushi Hashizume,[1] Masahisa Katsuno,[1] Haruhiko Banno,[1,2] Keisuke Suzuki,[1] Noriaki Suga,[1] Tomoo Mano,[1] Naoki Atsuta,[1] Hiroaki Oe,[3] Hirohisa Watanabe,[1] Fumiaki Tanaka[1] and Gen Sobue[1]

1 Department of Neurology, Nagoya University Graduate School of Medicine, Nagoya, 466-8550, Japan
2 Institute for Advanced Research, Nagoya University, 464-8601, Nagoya, Japan
3 Biometrics Department, Statistics Analysis Division 2, EPS Co., Ltd., 532-0003, Osaka, Japan

Correspondence to: Gen Sobue, MD,
Department of Neurology,
Nagoya University Graduate School of Medicine,
65 Tsurumai-cho, showa-ku,
Nagoya 466-8550, Japan
E-mail: sobueg@med.nagoya-u.ac.jp

Correspondence may also be addressed to: Masahisa Katsuno, MD
E-mail: ka2no@med.nagoya-u.ac.jp

Spinal and bulbar muscular atrophy is an adult-onset, hereditary motor neuron disease caused by the expansion of a trinucleotide CAG repeat within the gene encoding the androgen receptor. To date, several agents have been shown to prevent or slow disease progression in animal models of this disease. For the translational research of these agents, it is necessary to perform the detailed analysis of natural history with quantitative outcome measures and to establish sensitive and validated disease-specific endpoints in the clinical trials. To this end, we performed a prospective observation of disease progression over 3 years in 34 genetically confirmed Japanese patients with spinal and bulbar muscular atrophy by using quantitative outcome measures, including functional and blood parameters. The baseline evaluation revealed that CAG repeat length in the androgen receptor gene correlated not only with the age of onset but also with the timing of substantial changes in activity of daily living. Multiple regression analyses indicated that the serum level of creatinine is the most useful blood parameter that reflects the severity of motor dysfunction in spinal and bulbar muscular atrophy. In 3-year prospective analyses, a slow but steady progression was affirmed in most of the outcome measures we examined. In the analyses using random coefficient models that summarize the individual data into a representative line, disease progression was not affected by CAG repeat length or onset age. These models showed large interindividual variation, which was also independent of the differences of CAG repeat size. Analyses using these models also demonstrated that the subtle neurological deficits at an early or preclinical stage were more likely to be detected by objective motor functional tests such as the 6-min walk test and grip power or serum creatinine levels than by functional rating scales, such as the revised amyotrophic lateral sclerosis functional rating scale or modified Norris scale. Categorization of the clinical phenotypes using factor analysis showed that upper limb function is closely related to bulbar function, but not to lower limb function at baseline, whereas the site of onset had no substantial effects on disease progression. These results suggest that patients with spinal and bulbar muscular atrophy show a slow but steady progression of motor dysfunction over time that is independent of CAG repeat length or clinical phenotype, and that objective outcome measures may be used to evaluate disease severity at an early stage of this disease.

Received March 7, 2012. Revised May 3, 2012. Accepted May 10, 2012. Advance Access publication July 6, 2012
© The Author (2012). Published by Oxford University Press on behalf of the Guarantors of Brain. All rights reserved.
For Permissions, please email: journals.permissions@oup.com

Downloaded from http://brain.oxfordjournals.org/ at Nagoya University on March 31, 2013

Keywords: spinal and bulbar muscular atrophy; natural history; biomarker; random coefficient linear regression model; CAG repeat

Abbreviations: ALSAQ-5 = five-item amyotrophic lateral sclerosis assessment questionnaire; ALSFRS-R = revised amyotrophic lateral sclerosis functional rating scale

Introduction

Spinal and bulbar muscular atrophy, also known as Kennedy's disease, is an adult-onset, hereditary motor neuron disease characterized by muscle atrophy, weakness, contraction fasciculation and bulbar involvement (Kennedy *et al.*, 1968; Sobue *et al.*, 1989; Sperfeld *et al.*, 2002). The progression of neurological deficits is usually slow in spinal and bulbar muscular atrophy, with the average interval between the onset of symptoms and death being ~20 years (Atsuta *et al.*, 2006). Life-threatening respiratory tract infections due to bulbar palsy often occur in an advanced stage of the disease, resulting in premature death. In blood profiles, the elevation of serum creatine kinase levels is a characteristic blood finding of spinal and bulbar muscular atrophy and is occasionally detectable many years prior to the onset of clinical symptoms (Sorarù *et al.*, 2008; Chahin and Sorenson, 2009; Rhodes *et al.*, 2009). In addition, patients often have non-neurological conditions, such as hyperlipidaemia and diabetes mellitus (Barkhaus *et al.*, 1982; Dejager *et al.*, 2002; Sinnreich *et al.*, 2004).

Spinal and bulbar muscular atrophy is caused by the expansion of a CAG repeat, encoding a polyglutamine tract, within the first exon of the androgen receptor gene (La Spada *et al.*, 1991). CAG repeat numbers range among 38–62 in patients with spinal and bulbar muscular atrophy, whereas normal individuals have 9–36 CAG repeats (La Spada *et al.*, 1991; Fischbeck *et al.*, 1997; Atsuta *et al.*, 2006). To date, nine polyglutamine diseases have been identified: Huntington's disease, dentatorubral–pallidoluysian atrophy, spinocerebellar ataxia 1, 2, 3, 6, 7 and 17, and spinal and bulbar muscular atrophy. Although the clinical features vary for each disorder, corresponding to the pathological distribution of neurodegeneration, the symptoms generally appear in mid-life and progressively deteriorate until death from fatal complications (La Spada and Taylor, 2003). Although several studies showed that CAG repeat size correlated with the age of onset in polyglutamine diseases, including spinal and bulbar muscular atrophy, considerable controversy surrounds whether the length of the CAG repeat influences the speed of disease progression (Atsuta *et al.*, 2006; Orr and Zoghbi, 2007; Walker, 2007).

The androgen-dependent accumulation of pathogenic androgen receptor proteins in the nucleus of lower motor neurons is thought to be crucial in inducing neuronal cell dysfunction and eventual degeneration, and underlie the gender dependency in the manifestation of the disease (Schmidt *et al.*, 2002; Katsuno *et al.*, 2012). In mouse models of spinal and bulbar muscular atrophy, surgical castration delays disease onset and reverses the neuromuscular phenotype (Katsuno *et al.*, 2002; Chevalier-Larsen *et al.*, 2004). Similar effects emerged when these mice are treated with leuprorelin, a luteinizing hormone-releasing hormone agonist that reduces testosterone release (Katsuno *et al.*, 2003). In a phase II clinical trial, leuprorelin suppressed the accumulation of pathogenic androgen receptor and slowed the deterioration of motor function in patients with spinal and bulbar muscular atrophy (Banno *et al.*, 2006, 2009). However, in a large-scale phase III randomized controlled trial, the efficacy of leuprorelin on clinical endpoints was not clearly demonstrated, although it was suggested that early intervention might be beneficial (Katsuno *et al.*, 2010). Similarly, the 5α-reductase inhibitor dutasteride, which blocks the conversion of testosterone to dihydrotestosterone, did not show a significant effect in a phase II clinical trial (Fernández-Rhodes *et al.*, 2011). These results appear to be partly attributable to the characteristics of spinal and bulbar muscular atrophy, such as its notably slow progression, and the lack of established outcome measures for the evaluation of therapeutic efficacy. In slowly progressive neurodegenerative diseases, the efficacy of a disease-modifying therapy is difficult to detect in short-term trials (Rascol, 2009). To facilitate the development of disease-modifying therapy for spinal and bulbar muscular atrophy, it is necessary to have a detailed description of the natural history of the disease to design appropriate clinical trials and to evaluate drug efficacy in patients. However, there are limited published data on the natural history of spinal and bulbar muscular atrophy, particularly for objective and quantitative measures, mainly because of its rarity (Rhodes *et al.*, 2009; Hashizume *et al.*, 2012).

In the present study, we performed prospective, quantitative analyses of the natural course of the disease in 34 genetically-confirmed Japanese patients with spinal and bulbar muscular atrophy over 3 years. Our results demonstrated longitudinal progression of quantitative outcome measures such as motor functional scales and tests as well as serum levels of creatinine. Although CAG repeat size in the androgen receptor gene correlates with activity of daily living milestones, i.e. hand tremor, muscular weakness, requirement of a handrail, dysarthria and dysphagia; its effect on disease progression rate was not demonstrated using random coefficient linear regression models. The analyses using these models also revealed that objective motor function tests and the serum levels of creatinine, but not subjective functional scales, are sensitive measures to detect neurological deficits at an early or preclinical stage of spinal and bulbar muscular atrophy. In addition, our findings indicated that upper limb function closely related to bulbar function, but not to lower limb function in spinal and bulbar muscular atrophy, whereas the site of onset had no substantial effect on disease progression.

Materials and methods

Patients

A total of 34 male patients with a diagnosis of spinal and bulbar muscular atrophy were recruited and followed with no specific treatment. The inclusion criteria were as follows: (i) genetically confirmed male Japanese patients with spinal and bulbar muscular atrophy with more than one of the following symptoms: muscle weakness, muscle

Downloaded from http://brain.oxfordjournals.org/ at Nagoya University on March 31, 2013

atrophy or bulbar palsy; and (ii) patients who were 25–75 years old at the time of informed consent. The patients were excluded if they met any of the following criteria: (i) unable to attend periodic follow-up visits; (ii) unable to stand upright for 6 min without assistance; (iii) tachycardia (>120 beats/min) or uncontrolled hypertension (>180/100 mmHg); (iv) experienced angina pectoris or myocardial infarction; (v) severe complications, such as malignancy and heart failure; (vi) severe bulbar palsy or other neurological complications; (vii) medical history of allergy to barium; (viii) taken hormonal agents within 48 weeks before informed consent; (ix) castrated; and (x) participated in any other clinical trials before informed consent. All of the patients were followed in Nagoya University Hospital. The data were collected between January 2007 and February 2011.

This study adhered to the ethics guidelines for human genome/gene analysis research and those for epidemiological studies endorsed by the Japanese government. The Ethics Committee of Nagoya University Graduate School of Medicine approved the study, and all participants gave their written informed consent.

Activity of daily living milestones

The initial symptoms and onset of nine activities of daily living milestones were assessed to evaluate the clinical course of the disease as previously described (Atsuta *et al.*, 2006). The activity of daily living milestones were defined as follows: hand tremor (patient awareness of hand tremor), muscular weakness (initial patient awareness of muscular weakness in any part of the body), requirement of a handrail (patient was unable to ascend stairs without the use of a handrail), dysarthria (patient was unable to articulate properly and had intelligible speech only with repetition), dysphagia (patient choked occasionally at meals), use of a cane (patient used a cane constantly when away from home), use of a wheelchair (patient used a wheelchair when away from home) and development of pneumonia (patient developed pneumonia that required in-hospital care). We assessed the age at which the activity of daily living milestones first occurred by direct interview at the first evaluation, since the inter-rater reliability of this method has been validated (Atsuta *et al.*, 2006). The activity of daily living milestones that occurred before the initial examination were checked and analysed. In this study, the age at which muscular weakness first occurred was defined as age at disease onset.

Outcome measures

The outcome measures of this study consist of functional and blood parameters, which were measured every 6 months during the 3-year follow-up. We used the following functional parameters in the present study: the revised amyotrophic lateral sclerosis functional rating scale (ALSFRS-R), modified Norris scale (Limb Norris score and Norris Bulbar score), modified quantitative myasthenia gravis score, grip power, 6-min walk test, five-item amyotrophic lateral sclerosis assessment questionnaire (ALSAQ-5), timed walking test (15 ft) and pharyngeal barium residue.

The ALSFRS is a validated questionnaire-based scale that measures physical function in patients with amyotrophic lateral sclerosis performing activity of daily living [The ALS CNTF treatment study (ACTS) phase I–II Study Group, 1996]. The revised version of this scale, ALSFRS-R, was generated to improve the disproportion of weighting to the limbs and bulbar system compared with respiratory dysfunction. The ALSFRS-R was translated into Japanese and validated (Ohashi *et al.*, 2001). The ALSFRS-R is divided into five domains: bulbar-related (three items: speech, salivation and swallowing), upper limb-related (two items: handwriting, and cutting food and handling utensils), trunk-related (two items: dressing and hygiene, and turning in bed and adjusting bed clothing), lower limb-related (two items: walking and climbing stairs) and respiration-related (three items: dyspnoea, orthopnoea and respiratory insufficiency).

The modified Norris scale is another rating scale for amyotrophic lateral sclerosis, which consists of two parts: the Limb Norris Score and the Norris Bulbar Score. The former has 21 items to evaluate limb function and the latter has 13 items to assess bulbar function. Each item is rated in four ordinal categories, and thus the possible best score is 63 and 39, respectively. The original version was translated into Japanese and validated (Oda *et al.*, 1996).

The quantitative myasthenia gravis score is an objective measure to detect fatigue of enduring muscle power that was originally designed for myasthenia gravis (Besinger *et al.*, 1983). We used a part of the quantitative myasthenia gravis score that measures the muscle power of the extremities and neck flexion as a modified quantitative myasthenia gravis score. Therefore, the best possible score is 0 and the worst possible score is 15. Although this scale has not been previously validated in patients with spinal and bulbar muscular atrophy, the contents of the modified quantitative myasthenia gravis score are suitable for the evaluation of spinal and bulbar muscular atrophy symptoms, and we thus considered them to be applicable to this disease (Katsuno *et al.*, 2010).

Grip power was measured using an electronic hand dynamometer. The patients were instructed to keep their elbows at 90°, their forearms in neutral rotation and their wrists not flexed or pronated. The measurements were performed twice on each side and the larger value was adopted as the grip power on each side. Grip power has been recommended as an acceptable endpoint for amyotrophic lateral sclerosis clinical trials (James *et al.*, 1997).

The 6-min walk test is a popular clinical test that has been used to assess the functional capacity of gait. The distance travelled during 6 min, i.e. the 6-min walk distance is a parameter that evaluates the global and integrated responses of all the systems involved in walking, including the neuromuscular, pulmonary and cardiovascular systems. The validity of this test has been verified in various neuromuscular disorders, including spinal and bulbar muscular atrophy (Takeuchi *et al.*, 2008; Montes *et al.*, 2010).

The timed walking test measures the time required to walk 15 feet. It has been recommended as a test for amyotrophic lateral sclerosis clinical trials (James *et al.*, 1997).

The ALSAQ-5 is a subjective health measure that was designed to evaluate the quality of life in patients with amyotrophic lateral sclerosis. This questionnaire was developed from the original version (ALSAQ-40) using item reduction (Jenkinson *et al.*, 1999; Jenkinson and Fitzpatrick, 2001). The validity of the Japanese version of the ALSAQ-40 has been confirmed (Yamaguchi *et al.*, 2004).

Pharyngeal barium residue was examined to evaluate swallowing function. In the videofluorography examinations, the patients were instructed to swallow 3 ml of 40% w/v barium sulphate twice while standing. Pharyngeal barium residue was measured for the first 3 ml swallowed because the first residue directly affects the second one. Pharyngeal barium residue after initial swallowing was measured by two masked independent investigators according to standard procedures using a semiquantitative scale: 0, 2, 5, 10, 20, 30, 40, 50, 60, 70, 80, 90 and 100% (Logemann *et al.*, 1989, 2000; Katsuno *et al.*, 2010). Previous studies have shown high intra- and inter-rater reliability for the measurement of videofluorographic swallowing, although little is known about the reproducibility of this parameter (Kuhlemeier *et al.*, 1998).

Blood sampling was performed at an outpatient clinic without any fasting.

Downloaded from http://brain.oxfordjournals.org/ at Nagoya University on March 31, 2013

Longitudinal analyses

The data of the patients who were evaluated only once during the follow-up period were eliminated from the longitudinal analyses. Follow-up data were defined as the values of the last evaluation. The differences between baseline and follow-up were analysed using a paired *t*-test. The disease progression rate per year was defined as the difference between the baseline and follow-up data divided by the follow-up period (years).

Genetic analysis

Genomic DNA was extracted from peripheral blood of the patients with spinal and bulbar muscular atrophy using conventional techniques. PCR amplification of the CAG repeat in the androgen receptor gene was performed using a fluorescent-labelled forward primer (5′-TCCAG AATCTGTTCCAGAGGTGC-3′) and a non-labelled reverse primer (5′-TGGCCTCGCTCAGGATGTCTTTAAG-3′). The detailed PCR conditions were described previously (Doyu *et al.*, 1992). Aliquots of the PCR products were combined with loading dye and separated by electrophoresis using an autoread sequencer (SQ-5500; Hitachi Electronics Engineering). The size of the PCR standards was determined by direct sequencing, as described previously (Doyu *et al.*, 1992).

Statistics

Statistical analyses were performed using SPSS Statistics 17.0 (SPSS Japan Inc.) or SAS Software version 9.2 (SAS Institute). Descriptive variables such as the mean, median, standard deviation, standard error of the mean and range were used to summarize the quantitative measures. Spearman's correlation coefficient was used to assess the correlations between the age at the appearance of each activity of daily living milestone and CAG repeat number, and the baseline characteristics and disease progression rate. For multivariate analyses, stepwise multiple linear regression was first performed to select the best subset of covariates. Covariates that strongly correlated with each other (Spearmann's correlation coefficient > 0.7) were eliminated to avoid the multicollinearity that may affect the precise selection of factors. In the 'Results' section, only associations that were selected by stepwise analysis and found to be significant ($P < 0.05$) are shown.

In order to address the representative disease progression most effectively, random coefficient regression models were used as the primary statistical method to evaluate the longitudinal relationship of outcome measures (Laird and Ware, 1982). Although its mathematical formulation is somewhat different, the theory underlying these models is essentially the same as that for a traditional univariate repeated measures ANOVA (Searle, 1988; McLean *et al.*, 1991). Random coefficient regression models utilize familiar designs such as ANOVA, but their hypotheses and designs are related to regression lines rather than to single observations and can deal with random variation of entry scores and rates of progression among subjects. These models also attend to 'random effects', that is, unmeasured, uncontrolled sources of variability and have been used for analysing natural history of neurodegenerative diseases (Nandhagopal *et al.*, 2009). Ignoring random effects can increase the chance of declaring statistical significance in error because the pooling of intra-subject with inter-subject variability falsely reduces the estimate of the error of variance.

Factor analysis was performed using the baseline data of ALSFRS-R to classify the clinical phenotypes of spinal and bulbar muscular atrophy. We selected the factors with loadings that were >1, and performed a 'Varimax' rotation on these factors to maximize the number of variables with high loadings for each factor (Williams *et al.*, 2005). The loadings of each variable on both of these factors were plotted against each other, and two groups of variables in different areas of the plot were selected for further analyses.

Results

Patient demographics and blood profiles

A total of 34 patients with spinal and bulbar muscular atrophy were included (Table 1). The characteristics of the present study population, such as age at the first evaluation, age at onset and CAG repeat length, were similar to those of previous studies (Atsuta *et al.*, 2006; Katsuno *et al.*, 2010; Fernández-Rhodes *et al.*, 2011). Blood count and biochemical and hormonal profiles are shown in Table 2. The most characteristic observations of the blood tests were the elevated levels of creatine kinase and the decreased levels of creatinine. A total of 29 cases (85.3%) showed abnormalities in both parameters, whereas none had a normal value for both creatine kinase and creatinine. Aspartate and alanine aminotransferase were elevated above the reference range in ~70% of the patients. The total testosterone level was also elevated in 23.5% of the patients, while no case showed an abnormally low level of this hormone.

Activity of daily living milestones

The timing of activity of daily living milestones in this cohort was equivalent to that in a previous study (Supplementary Table 1) (Atsuta *et al.*, 2006). For instance, the age at onset of muscle weakness was between 22 and 66 years, which was preceded by hand tremor in most cases, and the intervals between the onset of weakness and the requirement of handrails for stair climbing were 0 to 18 years. As previously reported (Atsuta *et al.*, 2006), all of the milestones including the onset of muscular weakness were significantly correlated with CAG repeat length (Spearman's correlation

Table 1 **Clinical and genetic features of 34 patients with spinal and bulbar muscular atrophy at baseline**

Demographic	Mean ± SD (range)
Age at the first evaluation (years)	53.6 ± 12.6 (27–74)
Disease duration (years)	9.2 ± 5.3 (2–21)
Age at onset (years)	44.4 ± 12.6 (19–66)
CAG repeat length in the androgen receptor gene (number)	47.9 ± 4.0 (40–57)
Functional parameters	
ALSFRS-R	42.6 ± 4.1 (32–48)
Limb Norris score	55.9 ± 6.9 (39–63)
Norris Bulbar score	34.6 ± 4.3 (22–39)
Modified quantitative myasthenia gravis score	6.1 ± 3.4 (0–13)
Grip power	42.2 ± 13.5 (16.6–70.6)
6-Min walking distance	350 ± 130 (60–569)
ALSAQ-5	10.3 ± 3.7 (5–18)
Timed walking (15 ft)	4.48 ± 2.51 (2.29–13.08)
Barium residue	13.7 ± 17.5 (0–65)

Downloaded from http://brain.oxfordjournals.org/ at Nagoya University on March 31, 2013

coefficient = −0.568 to −0.713), except for three milestones, i.e. use of a cane, developed pneumonia and use of a wheelchair, which were experienced by less than seven patients (Supplementary Table 1).

Baseline data of outcome measures

To clarify the clinical parameters that are associated with disease severity, we investigated the correlations between the value of the clinical parameters and the following demographic and anthropometric variables: age at first evaluation, CAG repeat length, disease duration, age at onset and body mass index. We also examined whether the value of the functional parameters correlated with blood parameters which are often abnormal in patients with spinal and bulbar muscular atrophy (Table 2 and Supplementary material). As a result, age at the first evaluation, serum creatinine, HbA1c, prothrombin time and body mass index were selected by the stepwise analyses as candidate variables that reflected disease severity in the patients with spinal and bulbar muscular atrophy examined in the present study (Supplementary Table 2). The age at baseline was correlated with the scores in the functional rating scales and walking capacity. Moreover, the serum levels of creatinine were strongly correlated with all of the clinical parameters, except for the ALSAQ-5 and pharyngeal barium residue, suggesting that this parameter is likely to be the most reliable and valid blood parameter that reflects disease severity. By contrast, no correlation was detected between the functional parameters and creatine kinase, although it is thought to be the most characteristic biomarker of spinal and bulbar muscular atrophy (Chahin and Sorenson, 2009). The scatter diagrams also showed strong simple correlations between the serum creatinine and the clinical parameters at baseline (Fig. 1).

Longitudinal assessment of outcome measures

Based on the results of baseline correlations, we prospectively analysed the longitudinal change of the functional parameters and the serum levels of creatinine. The results of longitudinal observation showed a slow but steady disease progression in all of the outcome measures we examined, except for the quality of life score (ALSAQ-5) and swallowing function (barium residue after initial swallowing) (Table 3). We also performed sample size estimation using the outcome measures that showed significant longitudinal changes (Supplementary Table 3). The results demonstrated that the functional rating scales require a smaller sample size than objective measures, although a larger number of patients have to be enrolled in clinical trials of disease-modifying therapies that slow disease progression in comparison with those of symptomatic therapies expected to improve motor function.

Next, we investigated the correlations between the baseline characteristics, such as age at onset, age at the first evaluation, disease duration and CAG repeat length and the disease progression rate of the outcome measures that showed significant changes during the 3-year follow-up (Table 3). The baseline characteristics we evaluated did not correlate with the longitudinal changes of any outcome measure, suggesting that disease progression may not be affected by the characteristics of these patients (Supplementary Table 4).

Furthermore, we analysed the longitudinal data in terms of the disease duration in each patient. The score of each outcome measure was plotted over disease duration for each subject (Fig. 2). The trajectory for each subject was expressed with a connected line over the plot. We applied modelling processes to clarify the representative progression of spinal and bulbar muscular atrophy. To this end, linear multivariate regression analyses using random effects (random coefficient regression models) were utilized to model our longitudinal data since this model is robust to inter- and intra-individual variation and allowed the analysis of the repeated data of each subject (Deschaintre *et al.*, 2009; Nandhagopal *et al.*, 2009). In addition to the linear relationship, we also assessed non-linear models by adding a quadratic term of disease duration as an explanatory variable, and used exponentially decreasing models as an alternative description of the relationship. We evaluated the *P*-values of the quadratic term of estimate and Akaike's information criterion (Akaike, 1973) for

Table 2 Haematological profiles at baseline (n = 34)

Haematological test	Mean ± SD (range)	Reference range	Out of reference range (%)	
			Low	High
Total lymphocytes ($\times 10^3/\mu l$)	2.6 ± 0.7 (1.2–4.2)	1.5–3.5	2.9	11.8
Total protein (g/dl)	7.5 ± 0.5 (6.6–8.9)	6.7–8.3	2.9	2.9
Albumin (g/dl)	4.2 ± 0.3 (3.7–5.0)	4.0–5.0	20.6	0
HbA1c (l)	5.4 ± 0.8 (4.7–8.8)	4.3–5.8	0	14.7
Creatine kinase (IU)	969 ± 573 (144–2050)	62–287	0	91.2
Aspartate transaminase (IU/l)	46.2 ± 27.3 (23–159)	13–33	0	64.7
Alanine transaminase (IU/l)	57.7 ± 47.6 (17–272)	6–30	0	79.4
Uric acid (mg/dl)	5.5 ± 1.5 (2.5–9.3)	3.6–7.0	5.9	17.6
Testosterone (μg/dl)	7.4 ± 3.1 (3.7–15.0)	1.66–8.11	0	23.5
Creatinine (mg/dl)	0.45 ± 0.09 (0.22–0.66)	0.60–1.10	94.1	0
Prothrombin time (%)	101.4 ± 9.3 (85.0–129.2)	80–120	0	2.9
Activated partial thromboplastin time (%)	33.6 ± 2.8 (10.4–29.0)	80–120	14.7	32.4

Downloaded from http://brain.oxfordjournals.org/ at Nagoya University on March 31, 2013

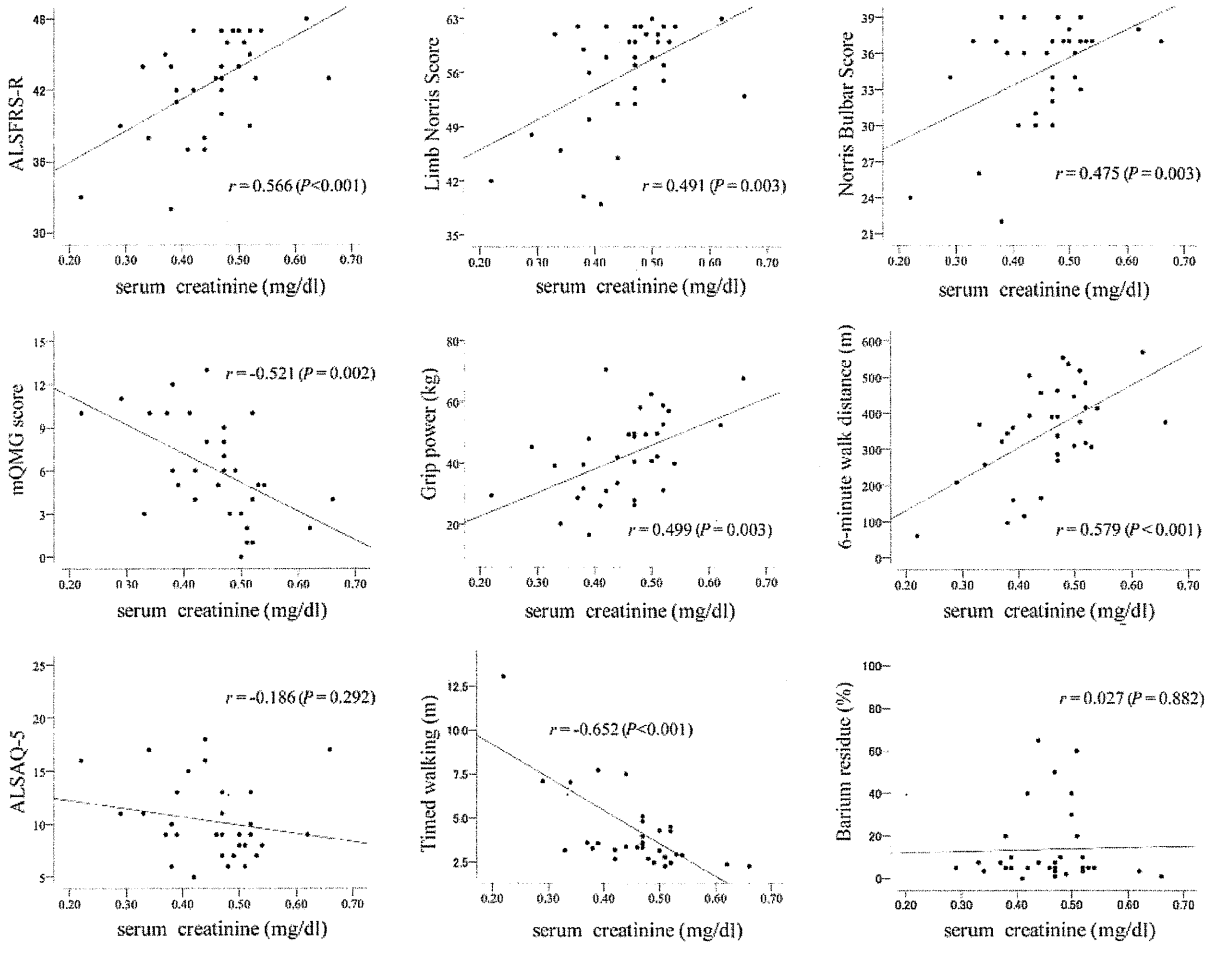

Figure 1 Simple correlations of serum creatinine levels with the outcome measures. Each outcome measure, other than barium residue, correlates well with the serum creatinine levels. mQMG = modified quantitative myasthenia gravis score.

Table 3 **Longitudinal change of outcome measures**

Clinical outcomes	Baseline, mean ± SD (range)	Follow-up[b], mean ± SD (range)	*P*-value[c]	Change per year[d], mean ± SD
ALSFRS-R ($n = 33$)[a]	43.0 ± 3.7 (33–48)	39.8 ± 4.0 (26–46)	<0.001	−1.1 ± 0.9
Limb Norris score ($n = 33$)	56.4 ± 6.4 (39–63)	49.7 ± 8.9 (27–62)	<0.001	−2.2 ± 1.6
Norris Bulbar score ($n = 33$)	34.9 ± 3.7 (24–39)	31.9 ± 4.4 (21–38)	<0.001	−1.0 ± 0.9
Modified quantitative myasthenia gravis score ($n = 32$)	5.9 ± 3.3 (0–13)	7.1 ± 3.4 (1–13)	<0.001	0.4 ± 0.5
Grip power ($n = 32$)	42.6 ± 13.8 (16.6–70.6)	36.5 ± 13.8 (14.0–66.0)	<0.001	−1.7 ± 3.0
6-min walking distance ($n = 32$)	360 ± 126 (60–569)	315 ± 136 (1–515)	<0.001	−20.3 ± 26.0
ALSAQ-5 ($n = 32$)	10.2 ± 3.7 (5–18)	11.2 ± 3.6 (5–16)	0.051	0.2 ± 1.2
Timed walking (15 ft) ($n = 32$)	4.36 ± 2.44 (2.29–13.08)	5.46 ± 4.26 (2.06–22.53)	0.004	1.00 ± 3.37
Barium residue (%) ($n = 29$)	13.1 ± 17.1 (1–65)	13.8 ± 16.9 (1–75)	0.796	0.2 ± 5.1
Creatinine ($n = 32$)	0.45 ± 0.09 (0.22–0.66)	0.41 ± 0.10 (0.19–0.58)	<0.001	−0.013 ± 0.030

a The numbers of patients whose data were analysed are shown. The data of patients who were evaluated once during follow-up were eliminated from the analysis.
b Follow-up data were defined as the value of the last evaluation.
c *P*-value for paired *t*-test.
d Change per year was defined as follows. [(Follow-up data) − (Baseline data)/(observational period (years)].
Barium residue = barium residue after initial swallowing.

Downloaded from http://brain.oxfordjournals.org/ at Nagoya University on March 31, 2013

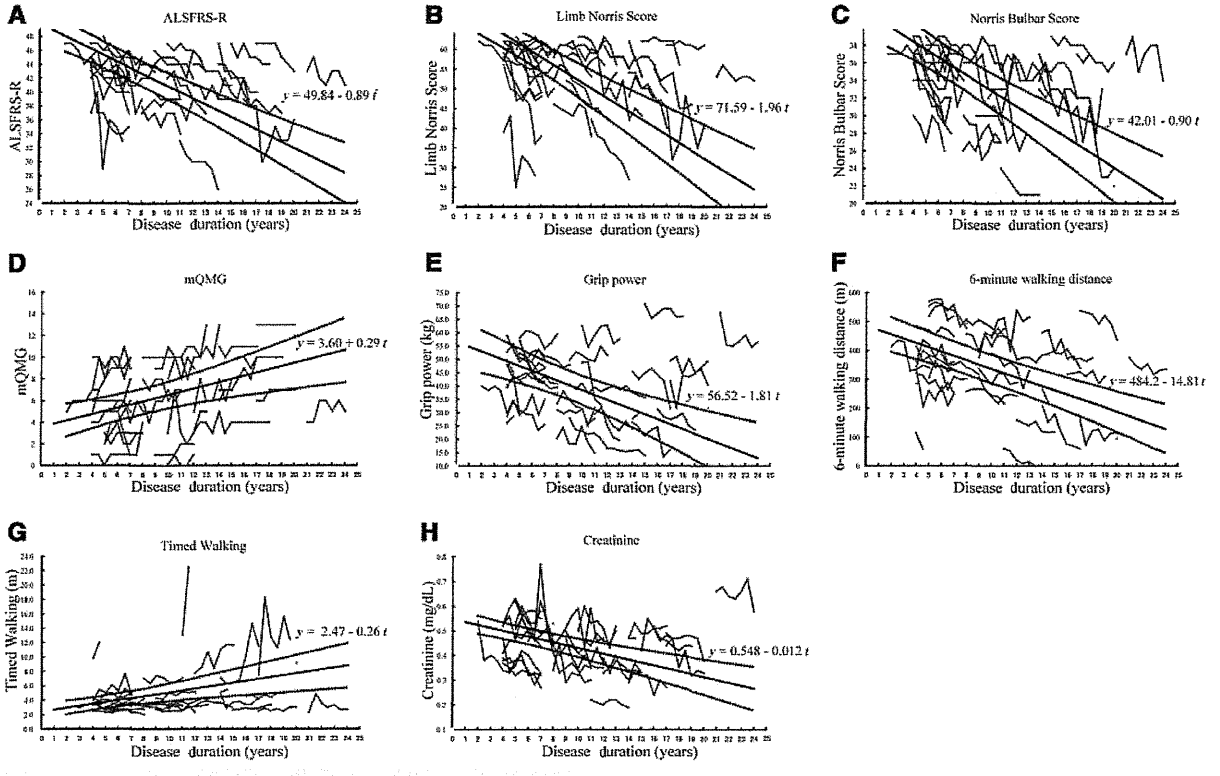

Figure 2 Longitudinal changes of outcome measures in consideration of disease duration. Neurological outcome measures and laboratory data obtained in each patient followed, according to disease duration, in years. The solid lines indicate representative disease progression over disease duration calculated by using random coefficient linear regression models. The broken curvilinear lines show the 95% confidence interval of these models. (**A**) ALSFRS-R; (**B**) Limb Norris score; (**C**) Norris bulbar score; (**D**) modified quantitative myasthenia gravis score (mQMG) (**E**) grip power; (**F**) 6-min walk distance; (**G**) timed walking; and (**H**) serum creatinine.

assessing fitness of these models. However, neither non-linear nor exponential models provided a substantially better fit than the linear models for the present data (Supplementary Table 5). In the analyses using the linear models, a fitted line was identified for all of the outcome measures, indicating a relentless deterioration of motor function in patients with spinal and bulbar muscular atrophy (Fig. 2). The linear models, shown by the solid lines in Fig. 2, were of the form $F(t) = a + bt$, where a, b and t were regression parameters to be estimated: t represented the disease duration; a represented the intercept at $t = 0$ (onset of symptoms); and b represented the disease progression rate. The broken curvilinear lines in each figure indicate the 95% confidence intervals of these models. In order to confirm that disease progression was not significantly affected by the patients' backgrounds, we split the patient population into two groups according to the level of their background variables, thereby generating two linear models. The results of this subgroup analysis considering CAG repeat length are shown in Supplementary Table 6. For all of the outcome measures, except for timed walking and creatinine, the progression rate was not significantly different, suggesting that disease progression is not strongly affected by CAG repeat length. Similarly, subgroup analyses according to the median value of age at onset and serum testosterone level also showed no substantial differences between the subgroups, except for the deterioration of grip power, which was faster than in patients with lower serum levels of testosterone (Supplementary Tables 7 and 8).

Figure 2 also showed that the individual behaviour of the chronological change had a large variation. Not only intra-individual but also interindividual variation was notably detected in each outcome measure. Thus we next investigated the characteristics of the patients whose baseline data of ALSFRS-R was below (Severe group) or above (Mild group) the curvilinear line of 95% confidence intervals (Fig. 2A). The results of this comparison showed that the patients of the mild group had better motor function despite longer disease durations compared with patients of the severe group, although there was no difference of the CAG repeat length in the androgen receptor gene or the age at the first examination between the groups. This indicates that factors other than CAG repeat size, such as physical capacity before the onset, might contribute to the variability of phenotypes in patients with spinal and bulbar muscular atrophy (Supplementary Table 9).

We next investigated the intercepts of the regression lines that corresponded to the estimated severity at clinical onset to identify clinical markers that are sensitive to the clinical changes during the early stage of the disease (Fig. 2). The intercepts of these regression lines were almost equal to or beyond the full score regarding

Downloaded from http://brain.oxfordjournals.org/ at Nagoya University on March 31, 2013